CR 73186

AVAILABLE TO THE PUBLIC

# EXPERIMENTS TO ESTABLISH CURRENT-CARRYING CAPACITY OF THERMIONIC-EMITTING CATHODES

Final Report

Contract No. NAS2-3379

AVSSD-0043-67-RR

Prepared for

National Aeronautics and Space Administration
Ames Research Center
Moffett Field, California

30 January 1967

Prepared by

Avco Corporation
Space Systems Division
Research and Technology Laboratory
Lowell, Massachusetts

FACILITY FORM 602

N68-16362
(ACCESSION NUMBER)

73
(PAGES)

CR-73186
(NASA CR OR TMX OR AD NUMBER)

(THRU)

1
(CODE)

25
(CATEGORY)

# EXPERIMENTS TO ESTABLISH CURRENT-CARRYING CAPACITY OF THERMIONIC-EMITTING CATHODES

Final Report

AVSSD-0043-67-RR

Prepared for

National Aeronautics and Space Administration
Ames Research Center
Moffett Field, California

Contract No. NAS2-3379

30 January 1967

Prepared by

Avco Corporation
Space Systems Division
Research and Technology Laboratory
Lowell, Massachusetts

Albert Tuchman
Project Manager

George Enos
Project Engineer

CONTENTS

I. INTRODUCTION..... 1

A. Program Objective..... 1
B. Program Organization..... 1
C. Technical Summary..... 2

II. FACILITY..... 4

A. Configuration..... 4
B. Instrumentation..... 9

III. TECHNICAL PROGRAM.....14

A. Materials.....14
B. Test Results--Pressure.....19
C. Test Results--Fall Voltage.....46
D. Summary of Results.....57

IV. CONCLUSIONS.....62

V. REFERENCES.....64

## ILLUSTRATIONS


Figure 1: Schematic of Cathode..... 5

2: Cathode Study Arc Facility..... 7

3: Photograph of Arc Facility.....10

4: Photograph of Arc Facility.....10

5: Schematic of Optical System.....12

6: Photomicrograph of BaO Material.....16

7: Photomicrograph of BaO Material.....16

8: Photomicrograph of BaO Material.....18

9: Photomicrograph of BaO Material.....18

10: Photomicrograph of BaO Material.....18

11: Schematic of Cathode Tip and Adaptor.....20

12: Typical Data Acquisition Sheet.....22

13: Photograph of Cathode Tip During Arc Operation, 400A, 3.5 psig.....23

14: Photograph of Cathode Tip During Arc Operation, 400A, 15 psig.....23

15: Photograph of Cathode Tip During Arc Operation, 400A, 30 psig.....24

16: Photograph of Cathode Tip During Arc Operation, 400A, 30 psig.....24

17: Cathode Diameter versus Chamber Pressure, 1/2-inch Thoriated Cathode.....26

18: Photograph of Cathode Tip After Testing, 100A.....27

19: Photograph of Cathode Tip After Testing, 200A.....27

20: Photograph of Cathode Tip After Testing, 300A.....28

Figure 21: Photograph of Cathode Tip After Testing, 400A.....28

22: Photograph of Cathode Tip After Testing, 500A.....29

23: Cathode Diameter versus Chamber Pressure, 1/2-inch Barium Oxided-Cathode.....31

24: Cathode Diameter versus Chamber Pressure, 1/2-inch Barium Calcium Aluminated Cathode.....32

25: Maximum Pressure versus Arc Current, 1/2-inch Cathodes.....33

26: Geometric Configuration of Conical-Cylindrical Tip.....36

27: Photograph of Cathode Tips.....37

28: Cathode Diameter versus Chamber Pressure, 1/4-inch Thoriated-Cathode.....38

29: Cathode Diameter versus Chamber Pressure, 1/2-inch Thoriated-Cathode.....39

30: Cathode Diameter versus Chamber Pressure, 1-inch Thoriated-Cathode.....40

31: Maximum Pressure versus Cathode Diameter, Thoriated-Cathodes.....41

32: Schematic of Hollow Cathode.....43

33: Photograph of Hollow Cathode After Testing, 500A, 3.5 psig.....44

34: Photograph of Hollow Cathode After Testing, 500A, 15 psig.....44

35: Photograph of Hollow Cathode After Testing, 500A, 30 psig.....45

36: Schematic of Button Cathode.....47

37: Photograph of Button Cathode Before Testing.....48

Figure 38: Cathode Fall Voltage versus Chamber Pressure, Thoriated-Cathodes.....49

39: Cathode Fall Voltage versus Chamber Pressure, Barium Oxided Cathodes.....51

40: Cathode Fall Voltage versus Chamber Pressure, Barium Calcium Aluminated-Cathodes.....52

41: Cathode Fall Voltage versus Chamber Pressure, 200 ampere.....53

42: Cathode Fall Voltage versus Chamber Pressure, 250 ampere.....54

43: Cathode Fall Voltage versus Chamber Pressure, 300 ampere.....55

44: Cathode Fall Voltage versus Chamber Pressure, 400 ampere.....56

45: Cathode Fall Voltage versus Chamber Pressure, Thoriated-Cathodes, 100 ampere.58

46: Cathode Fall Voltage versus Chamber Pressure, Thoriated-Cathodes, 200 ampere.....59

47: Cathode Fall Voltage versus Chamber Pressure, Thoriated-Cathodes, 300 ampere.....60

# I. INTRODUCTION

This document is the summary report of a program entitled "Experiments to Establish Current-Carrying Capacity of Thermionic-Emitting Cathodes," Contract NAS 2-3379, and summarizes the efforts under this contract by Space Systems Division, Avco Corporation for the period 11 January 1966 through 30 January 1967.

## A. PROGRAM OBJECTIVES

The primary objective of the present program has been that of obtaining data on the current-carrying capability of thermionic cathodes in a nitrogen atmosphere at pressure levels above 1 atmosphere. The experimental program has consisted of determining the maximum pressure level at which thermionic cathodes of different sizes, shapes and compositions may be operated at fixed current levels before catastrophic erosion of the cathode material begins.

## B. PROGRAM ORGANIZATION

The program originated from the Magnetoplasmadynamic Branch of the NASA Ames Research Center. Mr. C. Shepard was Project Manager for the Magnetoplasmadynamic Branch. Dr. A. Tuchman was Project Manager at Avco/Space Systems Division (Avco/SSD), and Mr. G. Enos was Project Engineer. The principal Avco/SSD participants and the areas in which they contributed are: Dr. Tuchman and Mr. Enos, Facility development; Mr. Enos, Mr. R. Krauss and Mr. C. Simard, Data Acquisition; Dr. Tuchman and Mr. Enos, Data Analysis; and Mr. T. Sturiale, Materials Fabrication.

## C. TECHNICAL SUMMARY

During the initial phase of this program, experiments were performed with the goal of determining the maximum steady-state current which can be carried by conical cathodes, as a function of ambient nitrogen pressure. The most noteworthy result of the initial tests was the observation of the cathode erosion phenomenon. It was found that for each fixed nitrogen pressure level, some cathode erosion was seen. As each new (higher) current level was set, material was continuously lost from the cathode for some initial time period, a new cathode tip diameter was established by the discharge, and the cathode then operated in a steady-state or equilibrium condition. No further erosion was seen thereafter for continued operation at the same, or lower, current and/or pressure levels. This process was repeated until some "critical" operating current (or pressure). At currents (or pressures) above this critical level, the material loss continued at a rapid rate, reducing, in some tests, the total cathode tip thickness to the order of only 1/16-inch. At that point, the arc was intentionally extinguished and the test was culminated.

On the basis of these first observations, the experimental program was reorganized in such a fashion as to permit the determination of the maximum pressure at which a given cathode can be operated before the onset of catastrophic erosion. The significant results of the test program are displayed as a graph of this maximum pressure versus the current level of operation.

The majority of tests were performed utilizing conical tip cathodes with $90^{\circ}$ included angle at the tip, and of fixed geometry. The cathodes were fabricated from tungsten impregnated with three different materials to determine the effects of the added material upon cathode performance. The materials used were thorium oxide, barium oxide, and barium calcium aluminate. A determination of the effects of size upon performance was made by comparing the performance of thoriated tips--all of the same geometric configuration--with diameters of 1/4-, 1/2- and 1-inch. Finally, several attempts were made to operate both cavity-type and button-type tips.

Several useful results were obtained under the program. Firstly, and of greatest importance, the addition of barium calcium aluminate was found to have a definitely beneficial effect upon cathode performance; cathode performance was markedly improved over that obtained with the other materials. Secondly, the use of larger diameter cathode tips did not always improve the operating characteristics of cathodes. For the fixed geometrical configurations employed in this program it was found that four 1/4-inch diameter cathode tips will carry more than a single 1/2-inch tip (same cross-sectional area), but that a 1/2-inch tip can carry more current than a 1-inch tip for certain operating conditions.

## II. FACILITY

### A. CONFIGURATION

A typical cathode tip, adaptor and holder are schematically shown in figure 1. The complete cathode unit shown was originally developed for an arc technology program which was being carried out at the inception of the present program. The copper holder consists essentially of two concentric tubes for coolant flow. An intermediate copper piece (adaptor plug) is brazed both to the holder and the tungsten tip, and is used to prevent coolant water from impinging directly upon the tungsten cathode tip. The cathode holder-copper plug bond is made with silver solder; the copper adaptor plug-tungsten tip joint is made by a gold braze. The fabrication procedure is as follows:

1. The copper adaptor plug, which is made from a section of slightly oversized diameter copper rod, is machined on one edge and gold brazed to the tungsten tip. Because of the extremely small difference between the gold braze temperature and the copper temperature, the copper tends to "sag" somewhat during the brazing operation. It is then machined on the face to be joined to the holder.

2. A silver solder joint is made at the copper-copper, holder to plug joint.

3. The oversized adaptor plug is machined to an outside diameter to match the OD of the tip and holder.

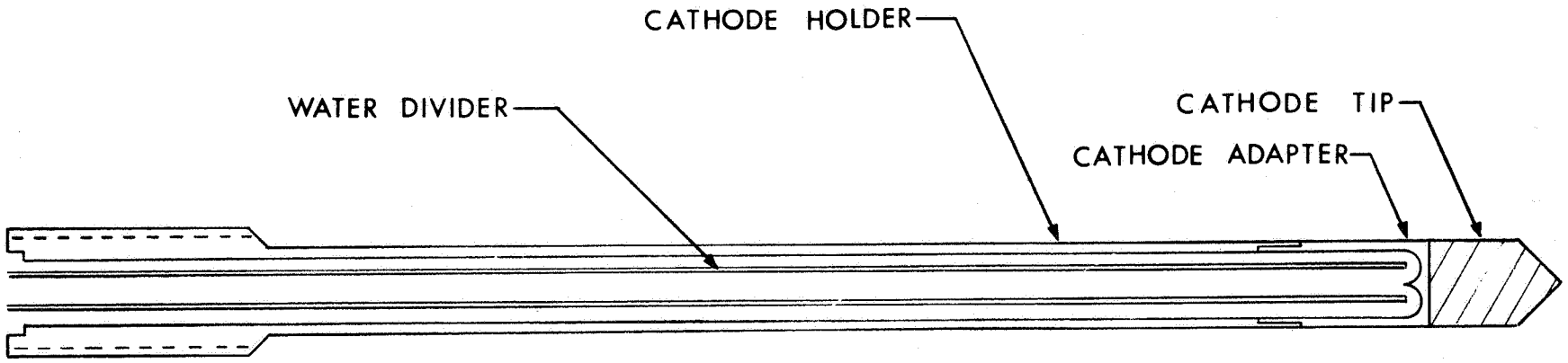


Figure 1: SCHEMATIC OF CATHODE

4. EAch time a tip replacement is desired, the silver solder joint is broken and a new tip-plug combination is silver bonded to the holder.

The tungsten-tipped cathode shown in figure 1 has an OD of 1/2-inches and is approximately 11 1/2-inches long. Similar cathodes have been fabricated in sizes of 1/4-inch OD and 1-inch OD and have been successfully used for the present program.

The mounting of the cathodes within the test facility is indicated in the schematic diagram of the facility shown in figure 2. The cathode is driven into and out of the facility by an electric motor so as to permit initiation of the electrical discharge at small cathode-anode separations and the subsequent withdrawal of the cathode tip to a position in line with the viewing port. Starting is accomplished at low pressure--Paschen's law breakdown--and the pressure is raised after the cathode tip is in its final position.

The facility has been operated at currents in the range of 100 to 1500 amperes and at chamber pressures of from 1 to 30 atmospheres. It consists of four distinct sections, all water cooled and electrically insulated from one another. A magnetic field is used to maintain a constant swirl of the arc attachment on the anode.

The anode section consists of a water cooled copper anode and constrictor. The anode housing has a 20 turn water cooled

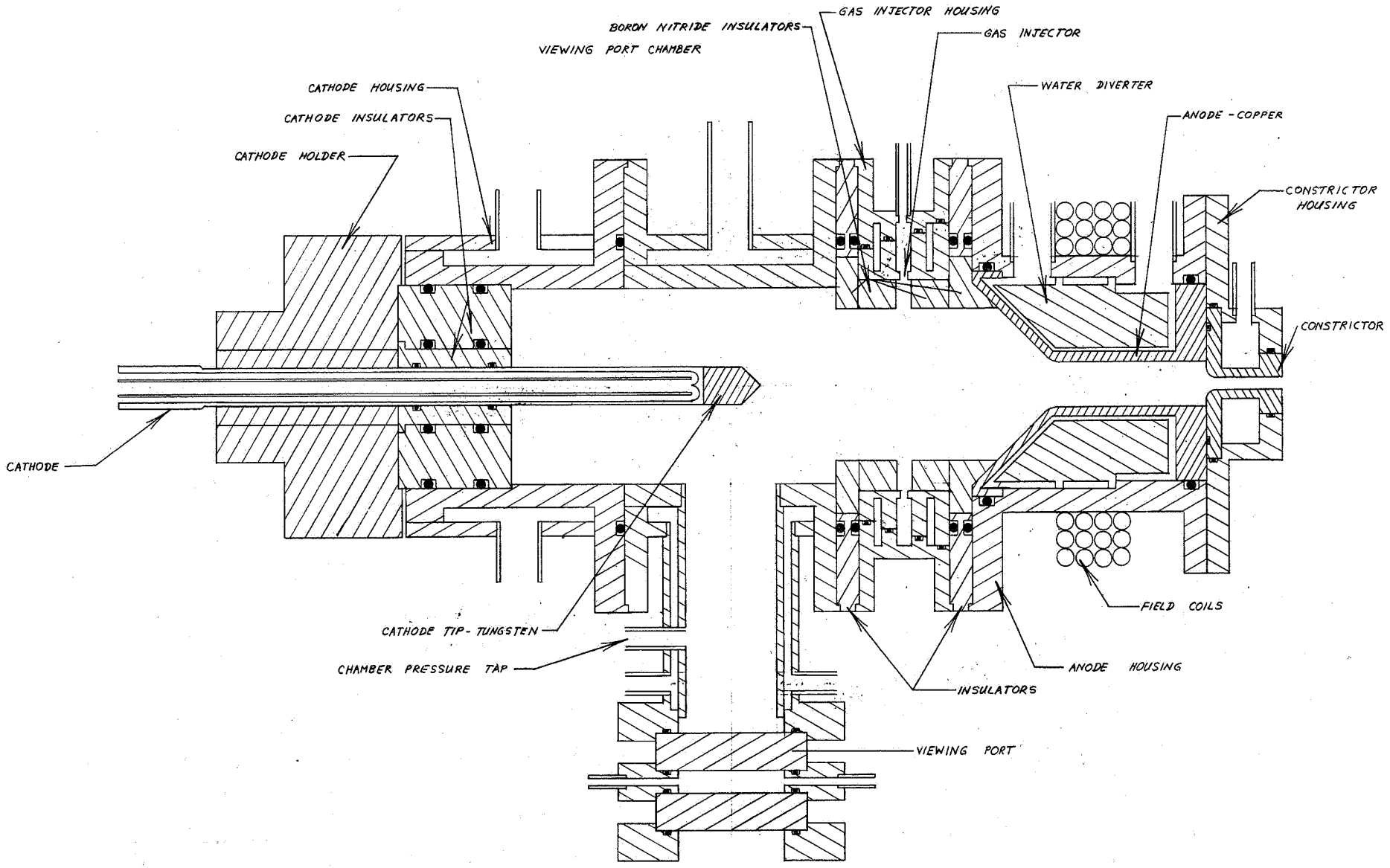


CATHODE STUDY ARC FACILITY
FIG. 2

copper magnet wound on its diameter. This magnet is powered by a 30 kw Miller power supply and was operated at a constant current, providing a constant field strength for all tests. The downstream side of the constrictor is run into a water cooled baffle (not shown in figure 2) and a flow control valve. This permits operation of the arc at high chamber pressures with a minimum of mass flow.

The gas injector section is located upstream of the anode and is electrically insulated from it by a micarta spacer and a boron nitride liner. Injection of the gas is through eight cylindrical ports tangent to the inside diameter of the housing and normal to the engine axis. These inlets are located approximately two inches downstream of the cathode tip so that the gas impingement upon the cathode is minimized.

The viewing section is also insulated from the gas injector by a micarta spacer. The viewing port is positioned so that visual observations of the cathode tip may be made at any time during the test. A camera lens (not shown in figure 2) is mounted in line with the viewing port and the cathode tip and is used for the magnification and projection of the cathode tip image onto a screen where a detailed study may be made. Chamber pressures are monitored through a tap located in the viewing port housing.

All sections of the arc facility are made gas and water tight by the use of o-rings and insulating pieces. The various gas and water inlets and outlets are metered with flow gauges,

pressure gauges and metering valves which are used to control pressure and mass flow rate in the arc. The cathode cooling water is monitored for both flow rate and temperature rise.

Power for the arc is supplied by two, 1/2-megawatt Perkin Power Supplies. Each of these rectifiers may be operated at 2000, 1000 or 500 amperes and 250, 500 or 1000 volts, respectively, and may also be connected in series or parallel, as desired.

Figure 3 and 4 show photographs of the arc test facility. Figure 3 shows the cathode driving mechanism (notched shaft on right side of photograph), the driving motor, the viewing port, water and electrical lines, and the projection lens mounted on a moveable slide. Figure 4 shows a close-up view of the viewing port and projection lens system. The exit baffle may be seen at the extreme left side of the photograph (water cooled copper tube).

B. INSTRUMENTATION

The various test and measurement equipments which are used to determine the performance of the arc test facility are: 1) the magnifying lens, 2) temperature measuring thermocouples, 3) current and volt meters, 4) pressure gauges. These are more fully described below:

1) Magnifying lens

The magnifying lens was a Wollensak 8-inch, f/5.6 telephoto lens. The lens was mounted in line with the viewing port and the cathode, and was used to project and magnify the image of the cathode tip onto a data sheet where a detailed

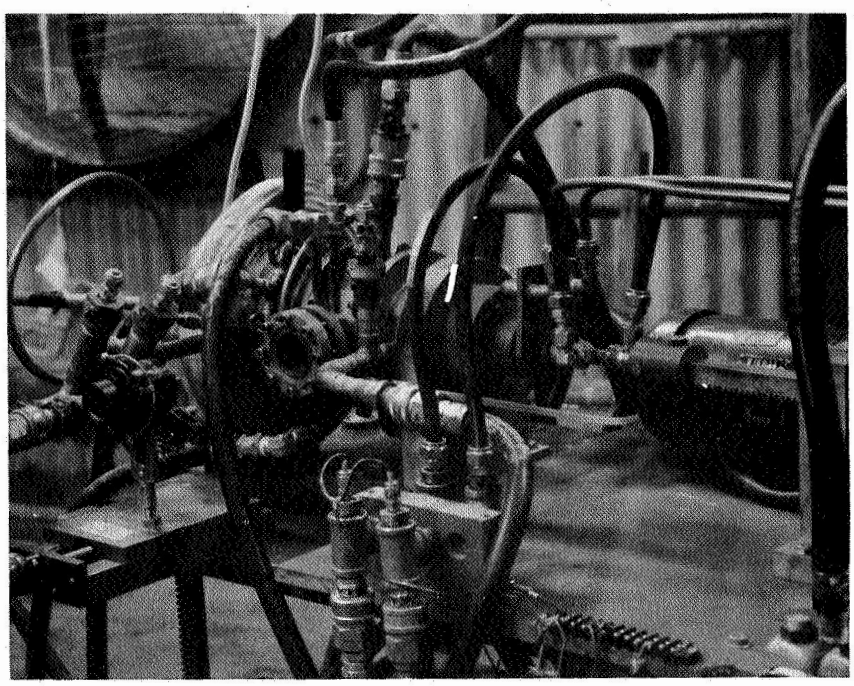

Figure 3: Photograph of Arc Facility

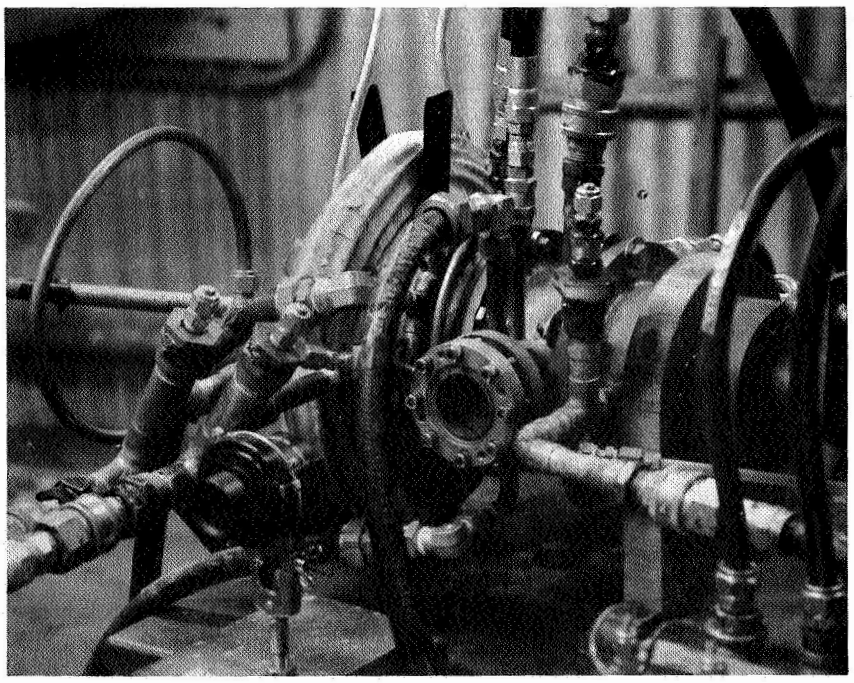

Figure 4: Photograph of Arc Facility

examination of the cathode shape could be recorded. The image of the cathode was magnified by approximately a factor of 22. Thus, an inaccuracy of as much as 1/4-inch in any given measurement upon the data sheet (an extraordinarily large inaccuracy) would represent an inaccuracy of only of the order of 10-mils on the actual cathode. Figure 5 shows a schematic diagram of the optical system.

2) Thermocouples

In order to accurately determine the effective voltage drop at the cathode, the power dissipated in heating the cathode is measured. The temperature rise of the cathode cooling water is measured by a differential Iron-Constantan thermocouple providing an output signal of 100 $\mu V/^{o}C$, and recorded on a Leeds and Northrup potentiometer with greater than 1 $\mu V$ accuracy. The temperature difference between water inlet and water outlet is converted to heat power when combined with the measured rate of water flow through the electrode.

3) Current, Voltage, and Flow Rate

Arc and coil current measurements are made with precision 50 MV shunt resistors and precision dc millivoltmeters. The millivoltmeters are fabricated by Assembly Products and the combination has a least count of 2 amperes and an uncertainty of 1/2% of full scale. The arc voltage is measured with a precision dc voltmeter. The water flow rates are measured using standard Fisher-Porter liquid flowmeters with 2% of full scale accuracy.

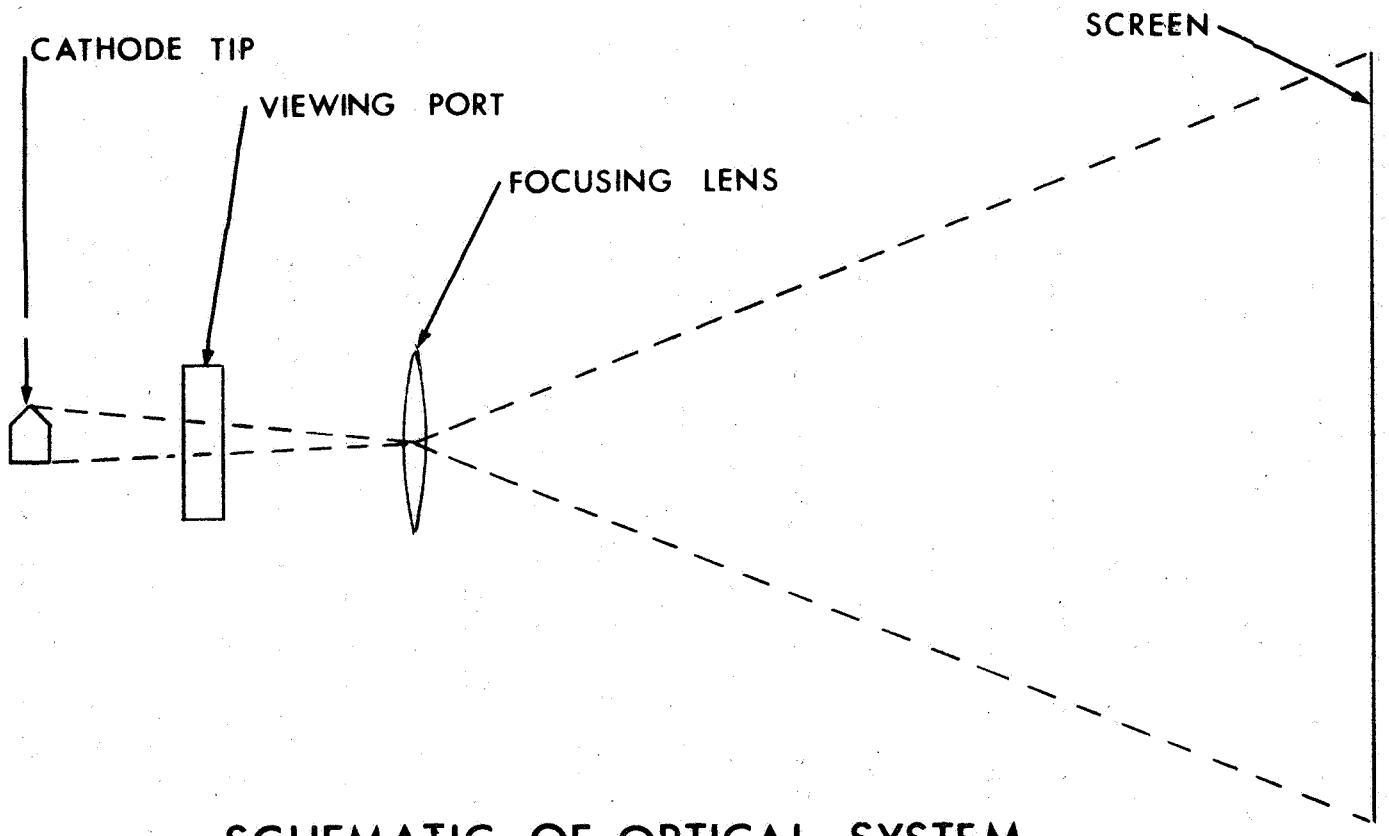


Figure 5: SCHEMATIC OF OPTICAL SYSTEM

4) Pressure Gauges

The arc chamber pressure is measured with a panel of Ashcroft Dura-gauge meters. The ranges covered by these gauges are 0-60 psig, 0-100 psig and 0-300 psig. These gauges have accuracies of 1/4% of full scale and least counts of .2, .5, and 1 psig, respectively. A 0-20 mm Hg gauge manufactured by Wallace and Tiernan is used to monitor the chamber pressure before the arc is started.

## III. TECHNICAL PROGRAM

### A. MATERIALS

The determination of the effects of material upon the current-carrying performance of thermionic-emitting cathodes was carried out using three impregnated-tungsten materials. The three materials, which in the remainder of this report will be called thoriated-, barium oxided-, and barium calcium aluminated-tungsten, respectively, had the following compositions.

1) Thoriated-Tungsten

Tungsten plus 2 percent by volume thorium oxide, with a density of at least 99% of the theoretical density of the composite material. This material was purchased for use in this program from both Sylvania Electric Products Co. and General Electric Co. Tests were performed to determine if differences in cathode performance resulting from the use of the different suppliers.

2) Barium Calcium Aluminated-Tungsten

This material was composed of tungsten impregnated with barium calcium aluminate. The material was purchased from Semicon Associates of Lexington, Kentucky, and was fabricated by infiltrating barium calcium aluminate into 80% dense tungsten billets to achieve a minimum weight pickup of 5%, with a uniform dispersion of the additive. The billets have been evaluated at Avco/SSD and have been determined to contain a uniform dispersion of the infiltrant. The material

obtained by the process outlined contains between 19 and 20% by volume of barium calcium aluminate, and has a density of at least 98.5% of the theoretical composite density of a uniform dispersion of the $(3BaO)(Al_2O_3)$ (BaO) (CaO).

3) Barium Oxided-Tungsten

The fabrication of this material was done at Avco. Five attempts have been made utilizing both hot pressing, and cold pressing and sintering techniques. The first attempt at hot pressing a 5 v/o BaO - 95 v/o W mixture was conducted at too high a temperature resulting in loss of BaO through melting and evaporation. During the hot pressing operation, the BaO was forced out of the tungsten matrix yielding a porous tungsten matrix.

In order to accelerate the densification process and permit lower fabrication temperatures, a small amount of nickel (.75 w/o) was added to act as a sintering aid. Hydrated nickelous nitrate $(N_i(NO_3) \cdot 6H_2O)$ was dissolved in water and 6-8 micron tungsten powder was added to form a slurry. After drying the mixture, the nickel compound was decomposed to nickel in a hydrogen atmosphere at 500°C. BaO was then added and the mixture was dry ball-milled for 4 hours. This material was then hot pressed at 1415°C and 4000 psi to yield a billet of 96% of the theoretical composite density. As is shown in figure 6 and 7, the BaO particles are uniformly dispersed throughout the tungsten matrix. An attempt at cold pressing

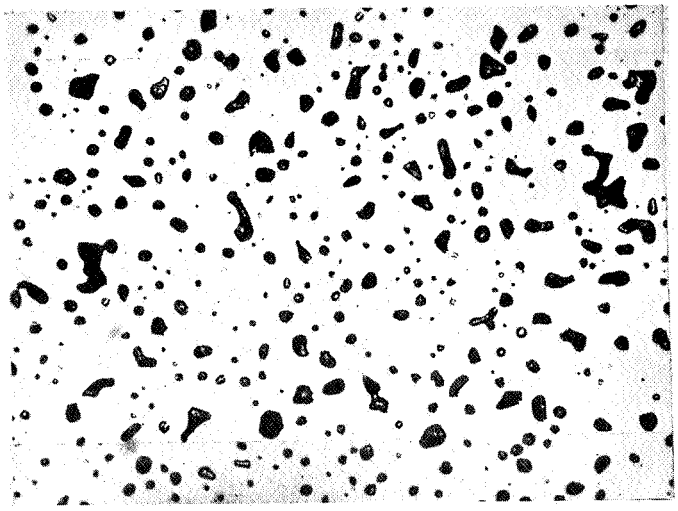

Figure 6: Mag. 500X
Unetched

BaO particles uniformly dispersed in hot pressed W Matrix

Composite 96% dense

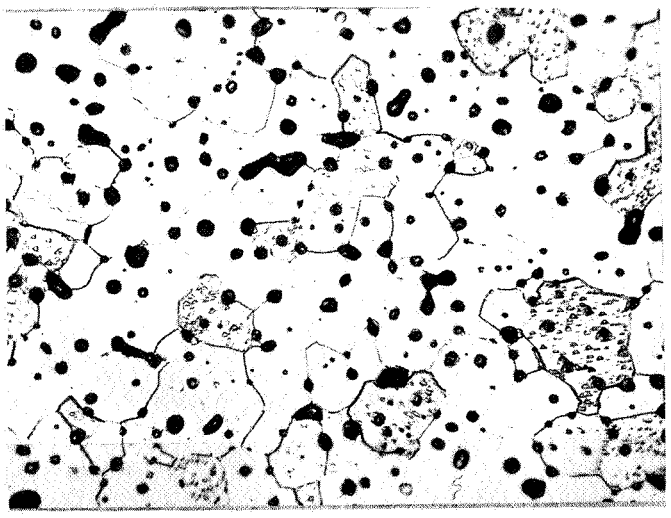

Figure 7 : Mag. 500X
Etched

Relative position of BaO particles with respect to grain boundaries. Dislocation etch pits evident in favorably positioned tungsten grains.

(at 50,000 psi) and sintering (at 1700°C) one-half inch diameter pellets yielded a density of 92% of the theoretical composite density (see figure 8).

The same procedure was utilized using 1 micron tungsten powder, that is, both hot pressing and cold pressing and sintering. However, a density of only 85.5% was obtained by hot pressing and the billet was extensively cracked (see figure 9). The results were somewhat better using the cold pressing and sintering technique (91.5% dense) although it was necessary to use a very carefully controlled time-temperature cycle to inhibit the cracking and reduce it to a minimum (see figure 10).

Two other attempts were made using both hot pressing, and cold pressing and sintering of 5 volume % BaO, 0.75 weight % Ni, with tungsten powder. Both a 75%-4 micron, 25%-1 micron and 80%-4 micron, 20%-1 micron tungsten powder mix were tried. Each of these attempts resulted in a sample of less than 95% of theoretical density.

A 1 1/4-inch thick, 5-inch square plate of barium oxided-tungsten was fabricated using 0.25 w/o nickel, 95 v/o tungsten in a 6.8 micron average size powder form, and 5 v/o barium oxide. The procedure followed was the first described above, that is, a slurry was formed and dried, the nickel compared was decomposed at 500°C in a hydrogen atmosphere, the barium oxide was added and the material was hot pressed at 1415°C

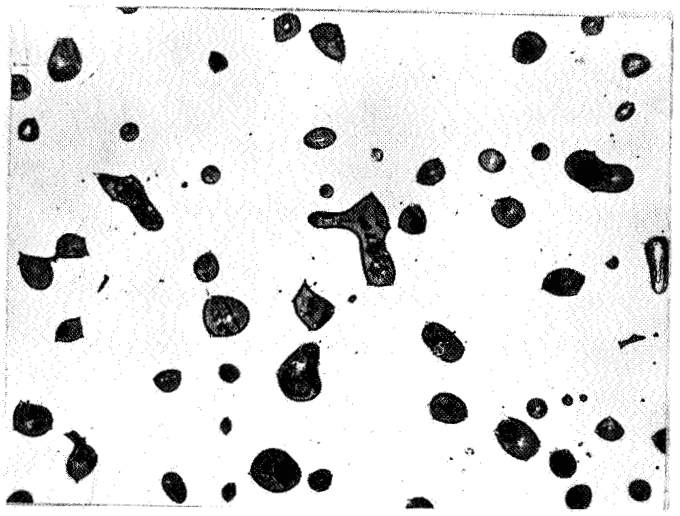

Figure 8: Mag. 500X
Unetched

Uniform dispersion of BaO particles in cold pressed and sintered W matrix. Note increase in BaO particle size due to agglomeration at higher temperatures and longer times.

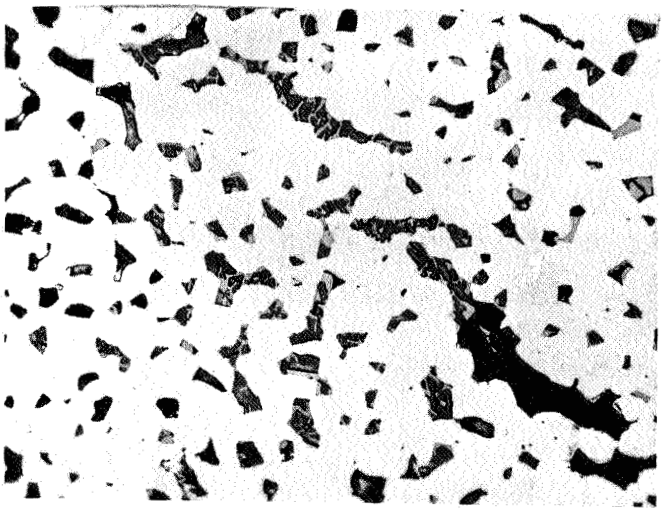

Figure 9: Mag. 500X
Unetched

Uniform dispersion of BaO particles in hot pressed W matrix. Note crack in lower right corner and angularity of BaO particles.

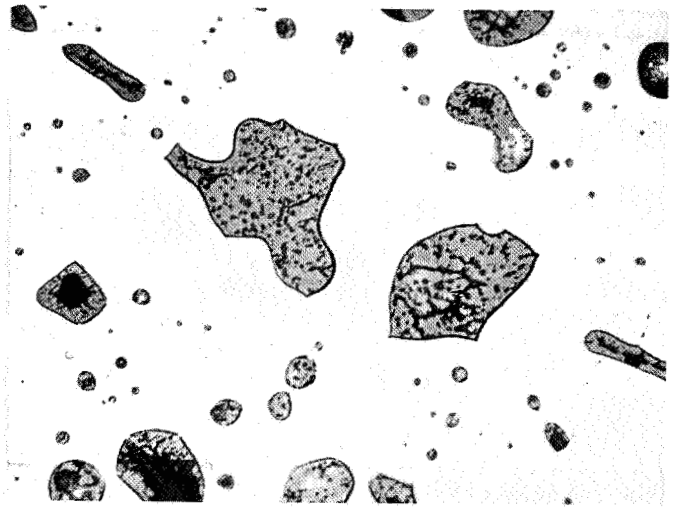

Figure 10: Mag. 500X
Unetched

BaO particles in cold pressed and sintered W matrix. Note nonuniform size of BaO particles. Larger particles due to agglomeration of BaO at higher temperatures and longer times during sintering.

at 4000 psi. The density obtained was 94.8% of theoretical composite density. It is not entirely clear why the density attained was below the 95% attained in the first test, but it is believed that this was due to the greatly increased sample size.

The plate was cut into 1-inch squares for machining into cathode tips. The squares were then resintered in an attempt to increase the material density. This process did not significantly increase the material density. The final density of the material used for the cathode program was 95.3% of the theoretical composite material density.

B. TEST RESULTS--PRESSURE

1. Effect of Cathode Material

Each of the three composites discussed above was fabricated into cone-cylinders. The cylindrical portion had a diameter of 1/2-inch, the conical tip had an included angle of 90° and was rounded at the tip to a 30 mil radius. The length of the cylindrical portion was 1/2-inch, resulting in an overall tip length of just under 3/4-inch. The tips were then brazed to copper plugs and copper holders as described in section II.A, above. Figure 11 shows a scale drawing of a cathode tip and its adapter plug.

For each material, the arc facility was operated at fixed current levels in the 100-500 ampere range, and the nitrogen pressure within the facility was increased in steps.

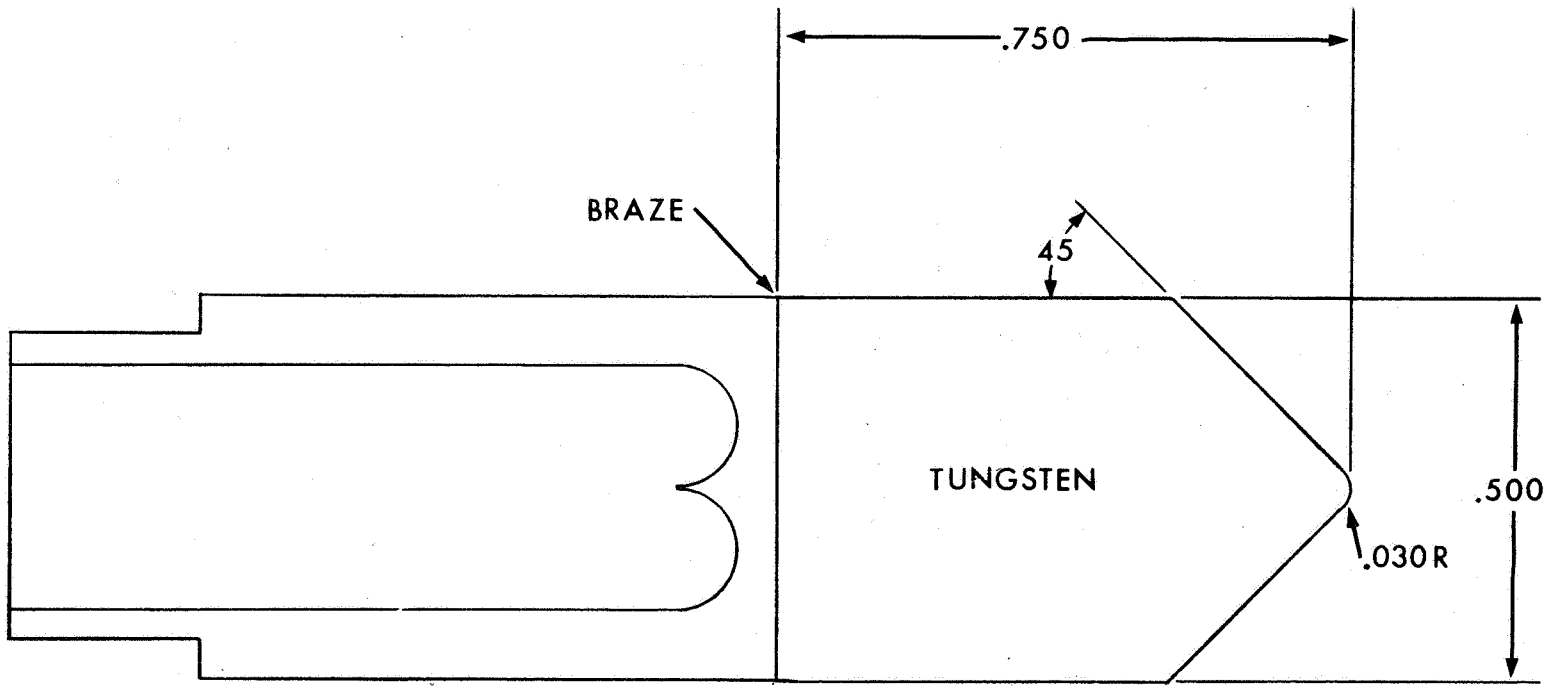


Figure 11: CATHODE TIP AND ADAPTER

At each set of current and pressure values of operation, the arc was permitted to operate until it reached complete equilibrium and the resulting equilibrium cathode tip shape was recorded, by hand sketch and occasionally by photograph, upon the data sheet. The recording process has been described above.

Figure 12 shows a typical data sheet on which the equilibrium cathode shapes for each pressure level have been recorded. The cathode image on an original data sheet is approximately 22 times life-size. Figures 13, 14, 15 and 16 show consecutive, chronological photographs of the data sheet taken during arc operation. The cathode erosion is readily seen in this series.

The recorded equilibrium cathode dimensions were transcribed from the magnified sketch and a plot of equilibrium cathode tip diameter versus chamber pressure was made for each operating current. It is to be recognized that the maximum tip diameter is limited to 1/2-inch; at the 1/2-inch cone diameter the conical portion of the tip joins into the 1/2-inch cylindrical portion of the tip (see figure 11). Moreover, the tip diameter at any position along the conical section is equal to exactly twice the axial tip length which has been eroded away. This last statement is, of course, due to the use of cathode tips with $60^{\circ}$ included angle at the apex of the cone.

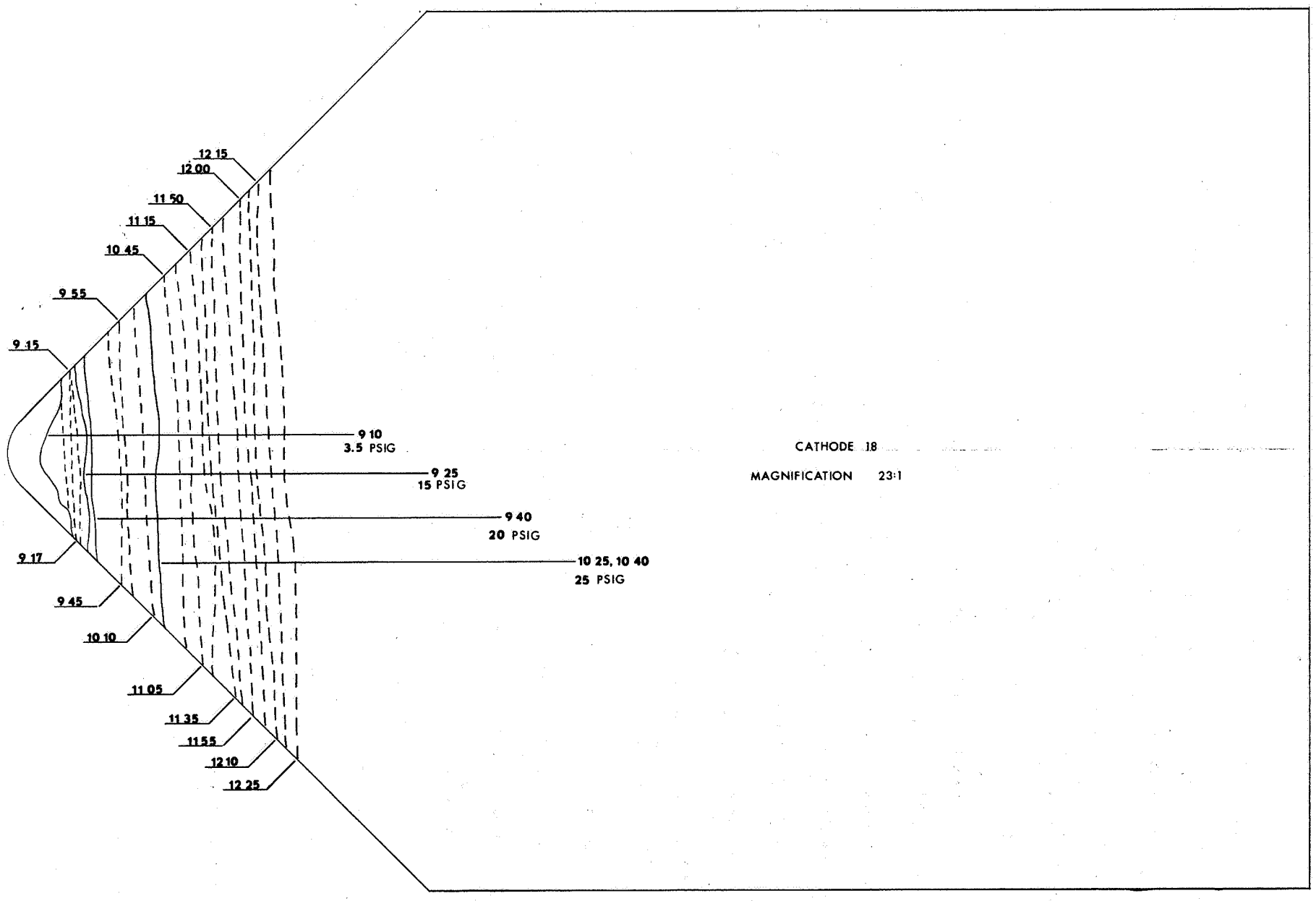


FIGURE 12: TYPICAL DATA ACQUISITION SHEET

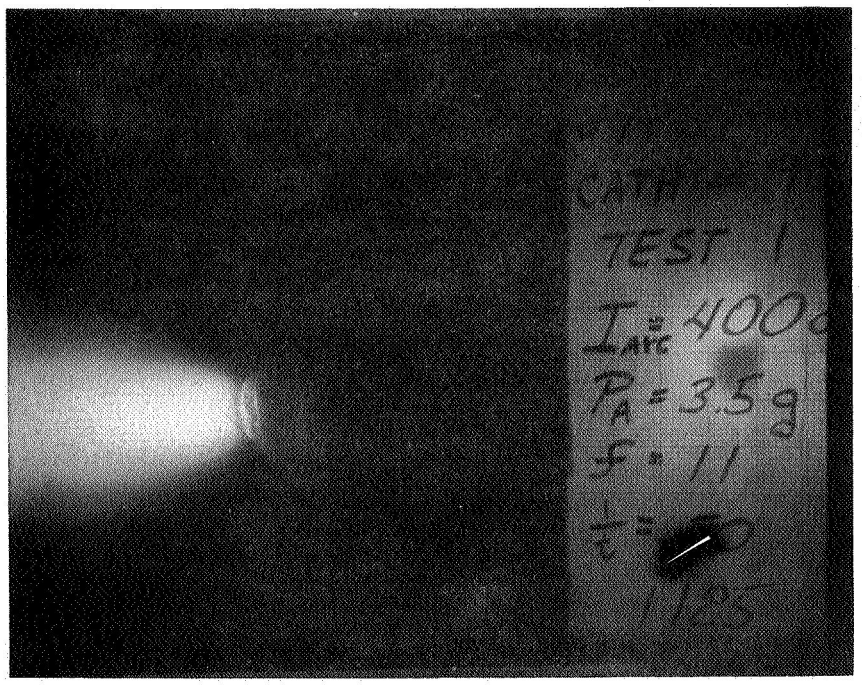


Figure 13: Photograph of Cathode Tip During Arc Operation, 400A, 3.5 psig

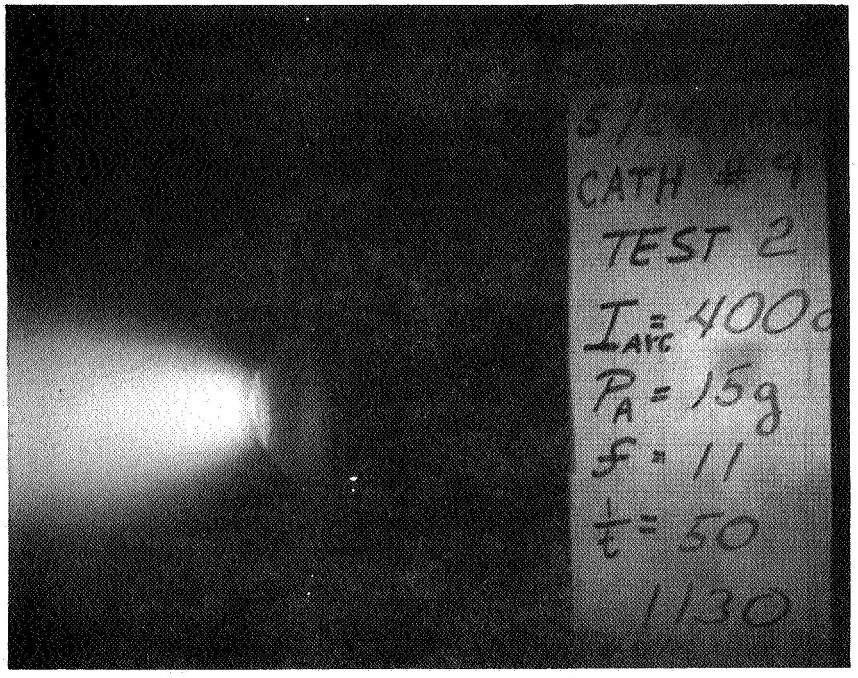


Figure 14: Photograph of Cathode Tip During Arc Operation, 400A, 15 psig

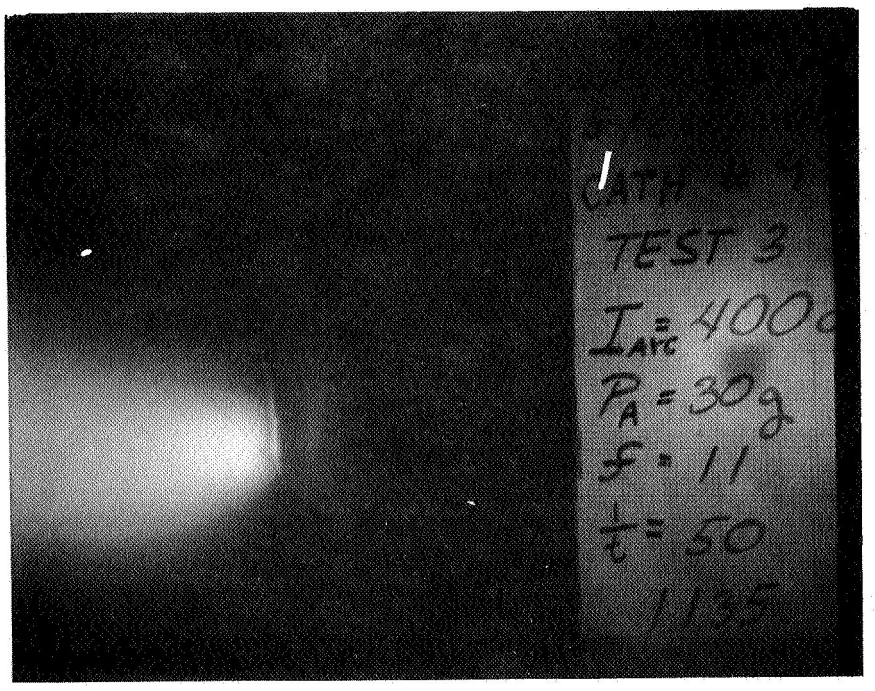


Figure 15: Photograph of Cathode Tip During Arc Operation, 400A, 30 psig

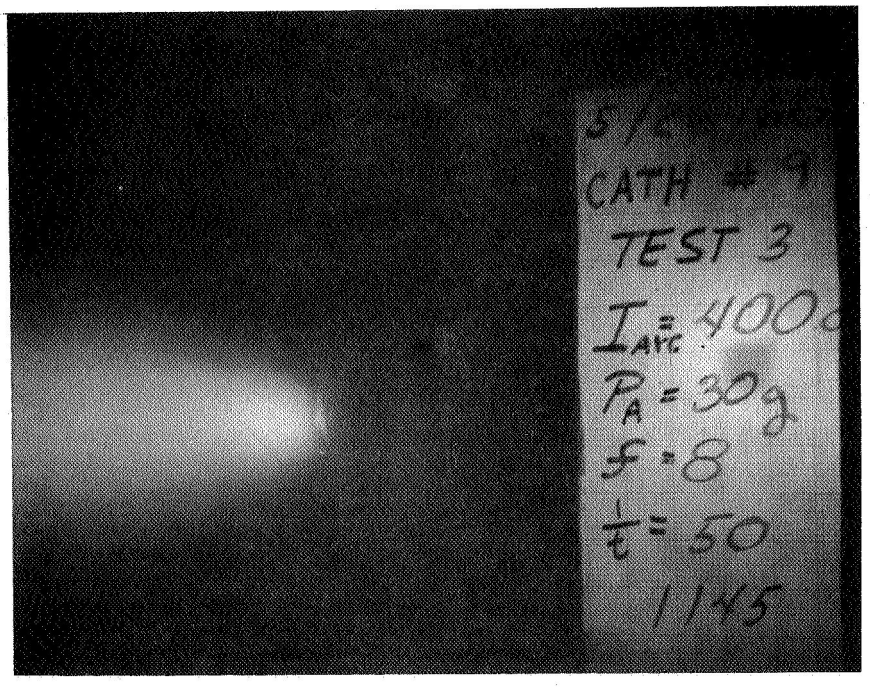


Figure 16: Photograph of Cathode Tip During Arc Operation, 400A, 30 psig

Figure 17 shows the equilibrium cathode diameter as a function of chamber pressure for 1/2-inch thoriated tungsten tips operated at various currents from 50 to 500 amperes. Two of the curves were obtained using thoriated tungsten obtained from General Electric Company; these are represented by the filled symbols on the figure. The open symbols represent the data obtained using the material purchased from Sylvania Electric Products Company. Also shown in the figure is a set of data obtained at an arc current of 200 amperes using ultra-high purity nitrogen as the ambient test gas.

The figure shows the general trends followed by each of the cathodes tested. At each operating arc current, the equilibrium cathode diameter increased with an increase in chamber pressure, until some critical pressure level was reached. Beyond the critical pressure level, catastrophic erosion began and no equilibrium diameter existed. This is indicated on the figure by the steeply rising dashed portion of each curve.

No differences of major significance are seen between the performance obtained with the cathodes fabricated from the materials obtained from the different suppliers. The use of high purity nitrogen gas also had no appreciable effects upon cathode performance.

Figures 18-22 show photographs of thoriated-cathodes after completion of tests at current levels of 100, 200, 300, 400 and 500 amperes, respectively. The flatness of the forward surface on each cathode is particularly noteworthy.

Figure 17: Cathode Diameter versus Chamber Pressure, 1/2-inch Thoriated Cathode

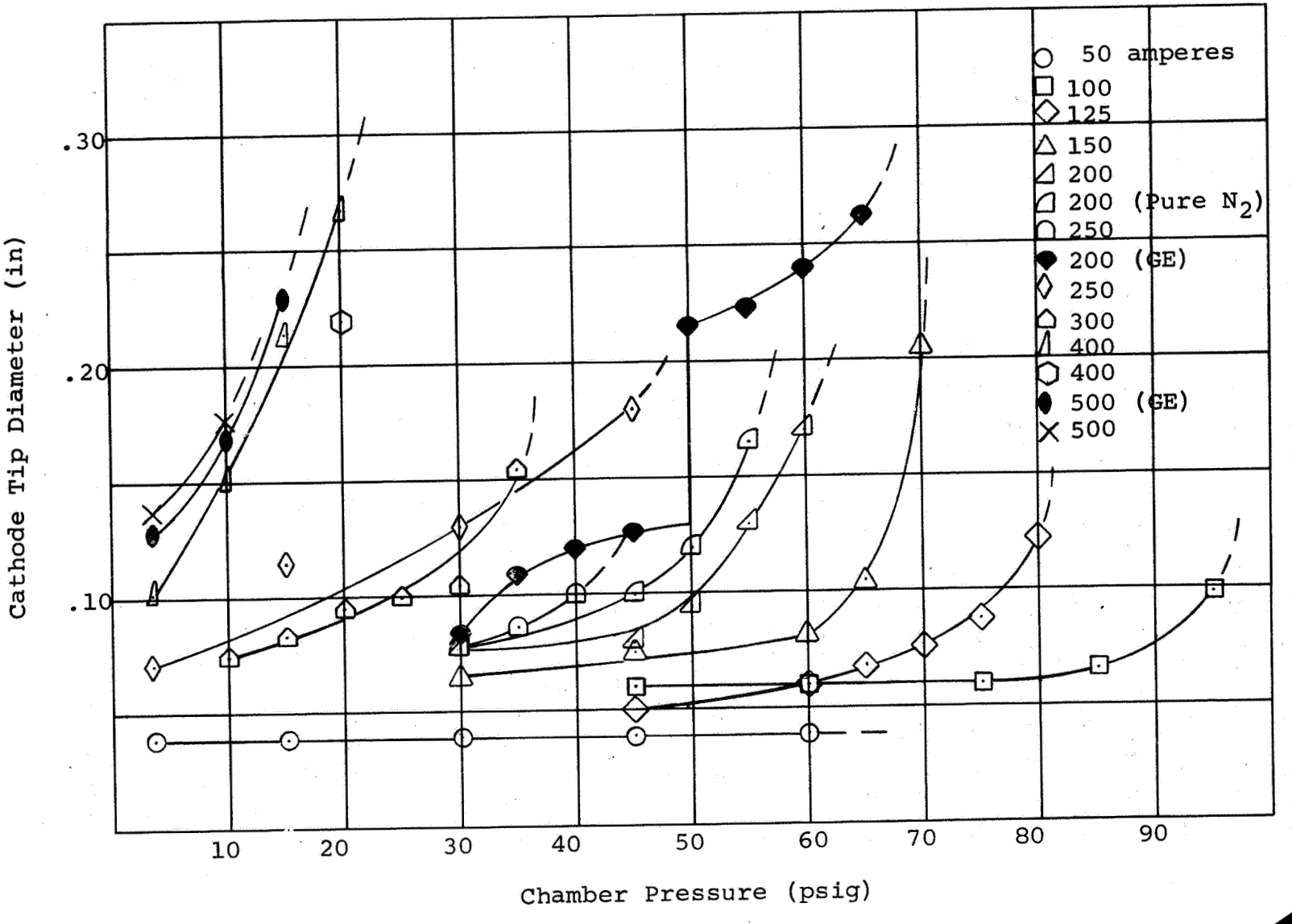

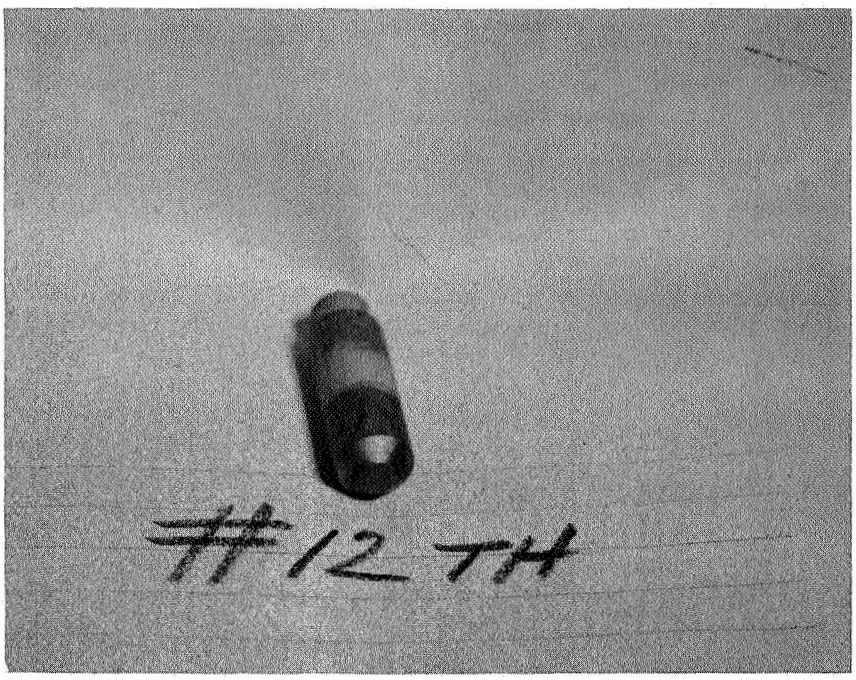


Figure 18: Photograph of Cathode Tip After Testing, 100A

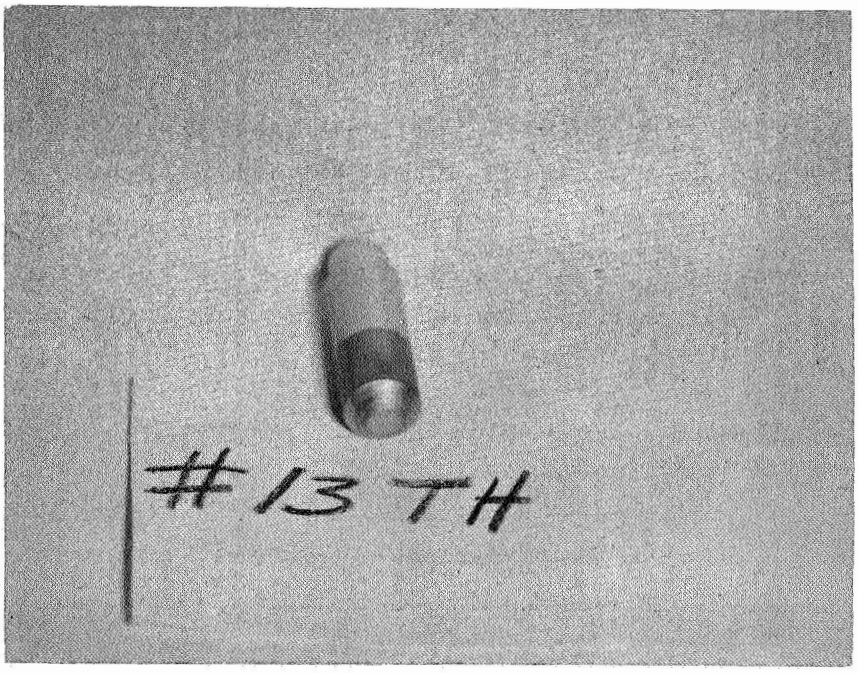


Figure 19: Photograph of Cathode Tip After Testing 200A

Figure 20: Photograph of Cathode Tip After Testing, 300A

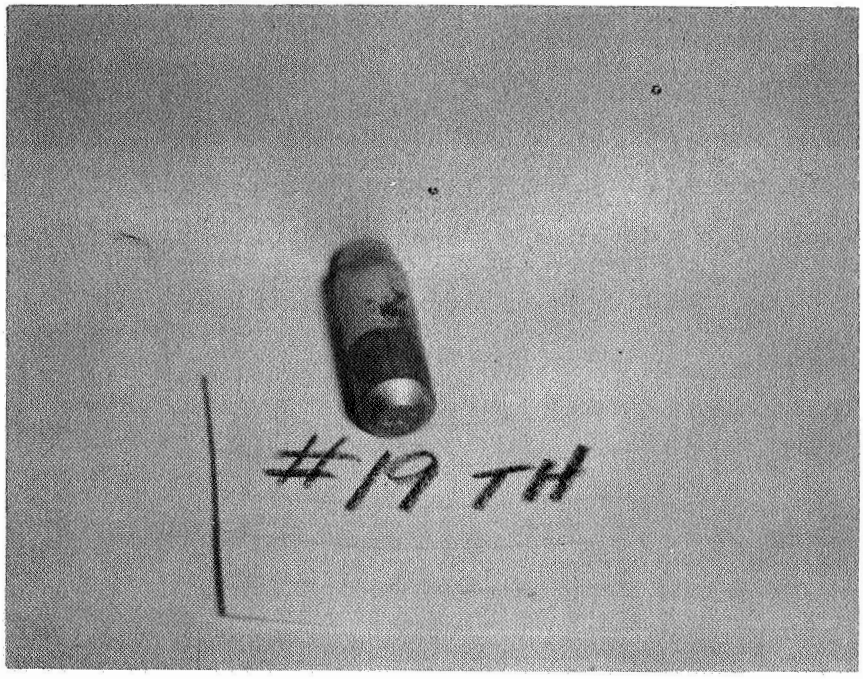


Figure 21: Photograph of Cathode Tip After Testing, 400A

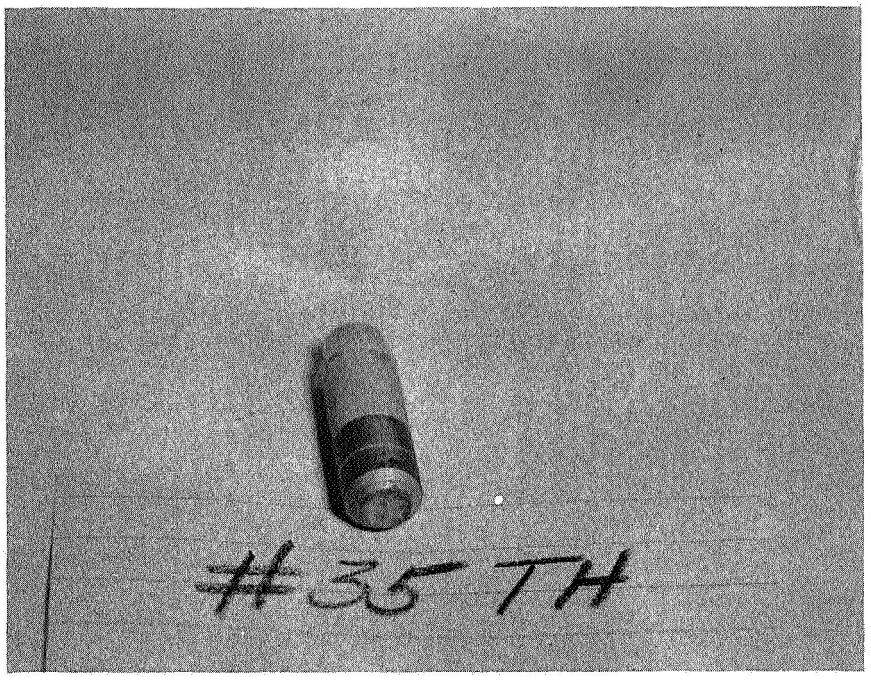


Figure 22: Photograph of Cathode Tip After Testing, 500A

Figure 23 presents the equilibrium cathode diameter as a function of chamber pressure for 1/2-inch barium oxided-tungsten, and figure 24 presents similar data obtained with 1/2-inch barium calcium aluminated-tungsten. The dependences shown exhibit the same general trends as those obtained with thoriated-tungsten cathodes (see figure 17).

The "critical" pressure has been defined, for the sake of simplicity and ease in data handling, as the greatest pressure at which an equilibrium cathode diameter exists. This maximum operating pressure could, as well, have been defined in terms of the position of the knee seen in most of the curves, but, for many of the curves, the ambiguity in determining this "point" is quite large, and the present definition was therefore utilized.

The maximum chamber pressure was determined from figures 17, 23 and 24, above, for each operating arc current. The resulting curves of maximum chamber pressure versus operating current are shown in figure 25 for the three materials. At an arc current of 100 amperes, the barium calcium aluminated-tungsten cathodes were operated at pressures above 20 atmospheres (~305 PSIA), as compared with a maximum pressure of only 7 atmospheres for the thoriated-cathodes and 13 atmospheres for the barium oxided-cathodes. Referring again to figure 24, it may be seen that the barium calcium aluminated-tungsten cathodes at 100 amperes never exhibited catastrophic erosion, even at 20 atmospheres, and that the maximum pressure

Figure 23: Cathode Diameter versus Chamber Pressure, 1/2-inch Barium Oxided-Cathode

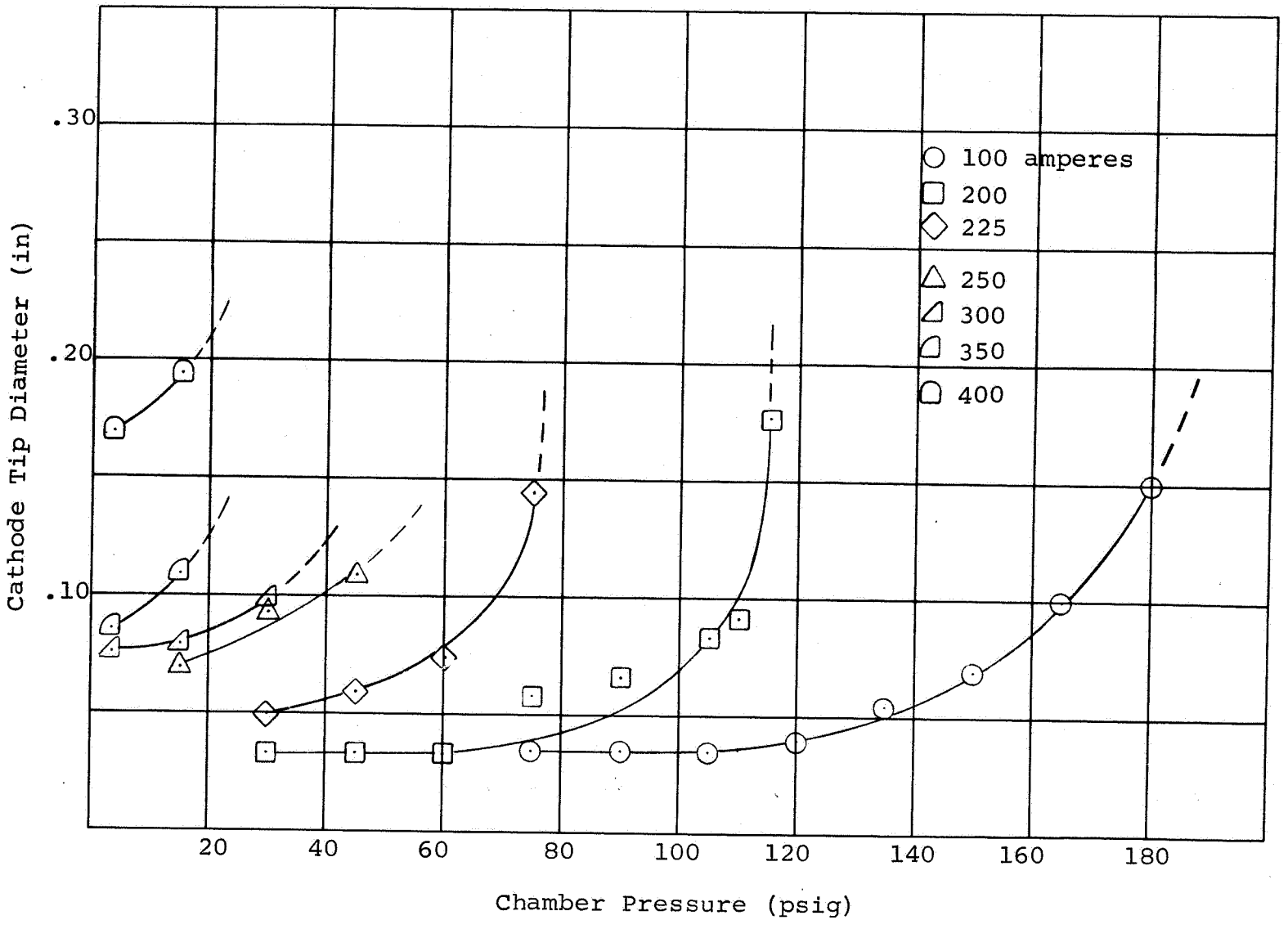

Figure 24: Cathode Diameter versus Chamber Pressure, 1/2-inch Barium Calcium Aluminated Cathode

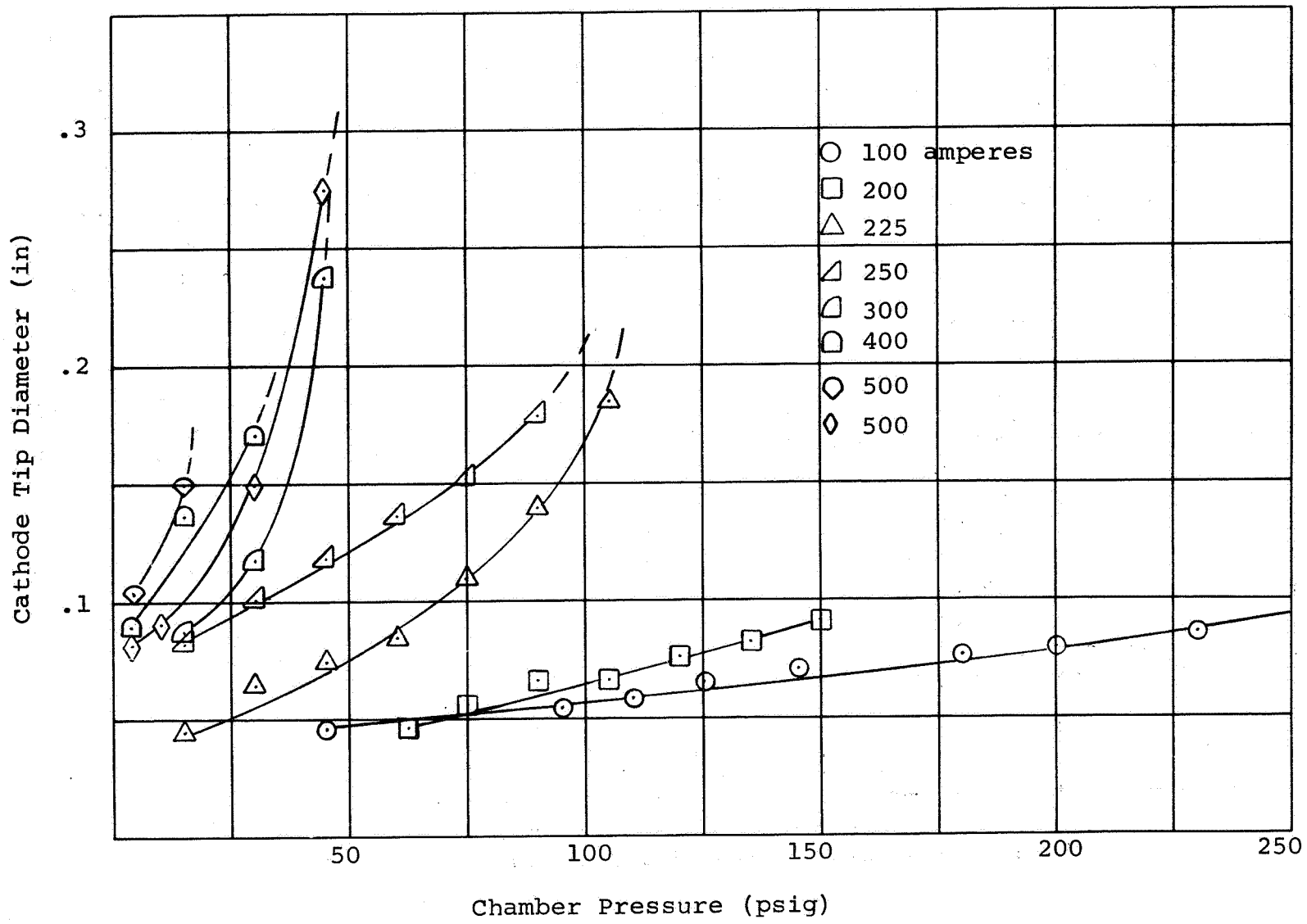

Figure 25: Maximum Pressure versus Arc Current, 1/2-inch Cathodes

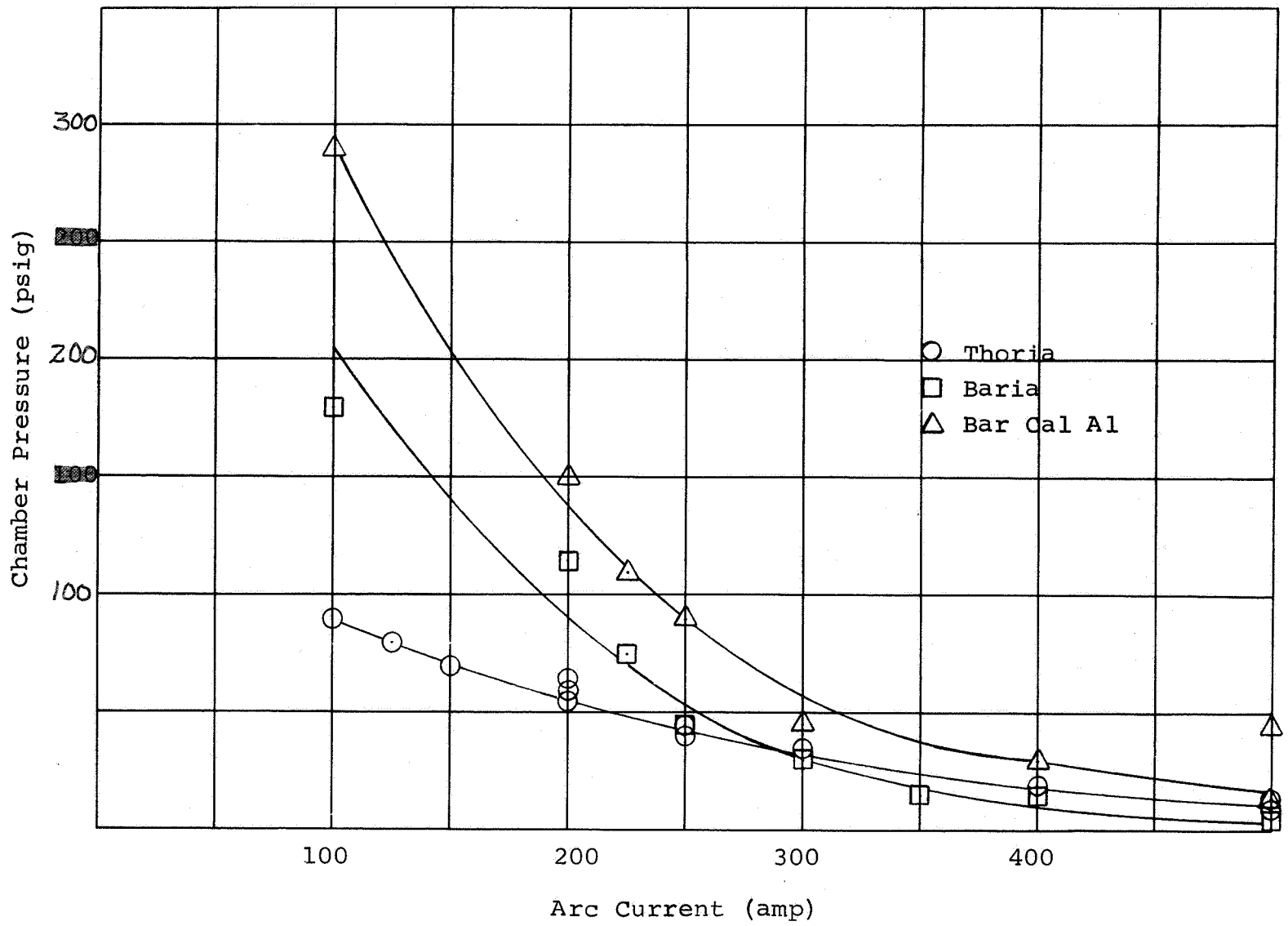

shown on figure 25 is really a lower limit on the actual value of the maximum pressure.

As seen from the figure, as the operating current was increased, the relative performance improvement obtained with the barium calcium aluminated-cathodes was reduced, but, at least up to 500 amperes, superior performance was always obtained with the barium calcium aluminated-tungsten cathodes than with either of the other two materials.

Of the three materials, the barium oxided tungsten exhibited the greatest "scatter" in the performance data obtained, particularly at the lower current operations. It also showed the rapid degradation in performance at increased current levels and, for currents above approximately 250 amperes, did not perform as well as thoriated-tungsten cathodes.

On the basis of the data shown in figure 25, there is little doubt that the most advantageous cathode performance, at least at arc currents of up to 500 amperes, is obtained using barium calcium aluminated-tungsten as the cathode material.

2. Effect of Cathode Size

In order to completely evaluate the effects of cathode size on current-carrying performance, the geometry for each cathode diameter should be varied to optimize its performance characteristics. This would involve varying both the length of the cylindrical portion of the cathode and the included angle at its tip. The present program was limited to a study

of the effects of cathode size for a fixed geometrical configuration. Each cathode had a $90^{\circ}$ included angle at its tip, and the cylindrical portion was fixed to have a length equal to its diameter. This had the effect of fixing the overall cathode length, from its tip to the base of its cylindrical portion, to be 1 ½ times as great as its diameter (refer to figure 26). Figure 27 shows a photograph of typical cathodes of the three sizes, before testing.

In order to insure that no other effects were operating to introduce performance differences, each of the cathodes used for this portion of the program was fabricated from thoriated-tungsten. Three different diameters were used; all materials utilized for this portion of the program were purchased from General Electric Co. and were tested for uniformity of composition and density. The densities were found to vary from one piece of material to the next by less than 3 parts per thousand (typically 19.01-19.05). The theoretical density of the composite is 19.21 (19.3 x .99 + 10 x .01) so that each sample piece utilized had a density of 99% of the theoretical composite density. Figures 28, 29 and 30 present the plots of equilibrium cathode diameter versus chamber pressure obtained for the ¼-inch, ½-inch and 1-inch sizes, respectively.

The same definition of maximum chamber pressure has been employed to obtain the curves of figure 31. The figure presents the maximum chamber pressure at which the different size cathodes may be operated; the different symbols represent the different arc current levels of operation.

The most striking feature of the curves shown in the figure, is their apparent maximum at, or near, the ½-inch cathode diameter

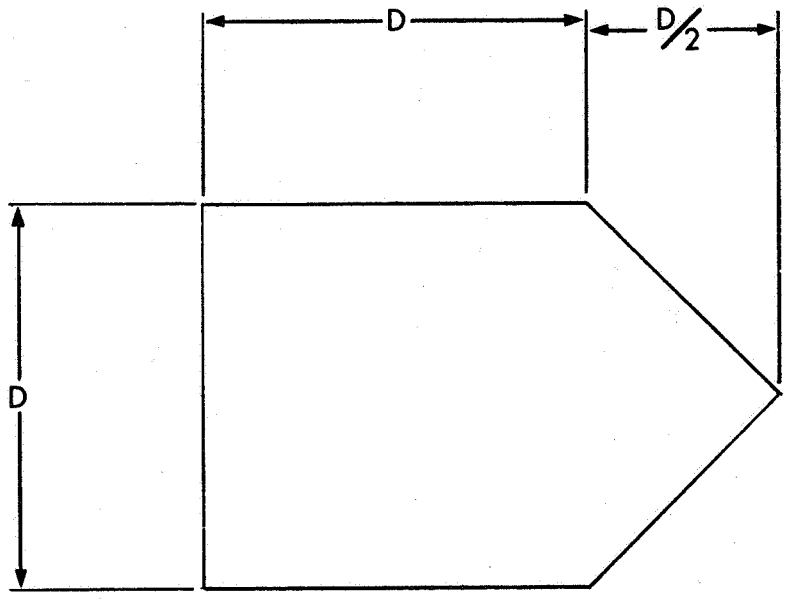


Figure 26: GEOMETRIC CONFIGURATION OF CONICAL—CYLINDRICAL TIP

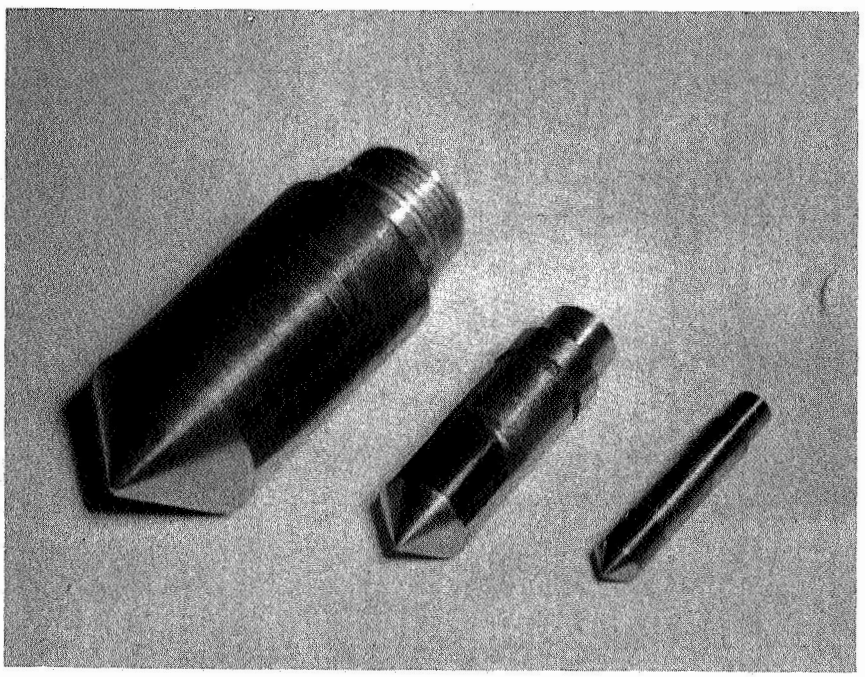

Figure 27: Photograph of Cathode Tips

Figure 28: Cathode Diameter versus Chamber Pressure, 1/4-inch Thoriated-Cathode

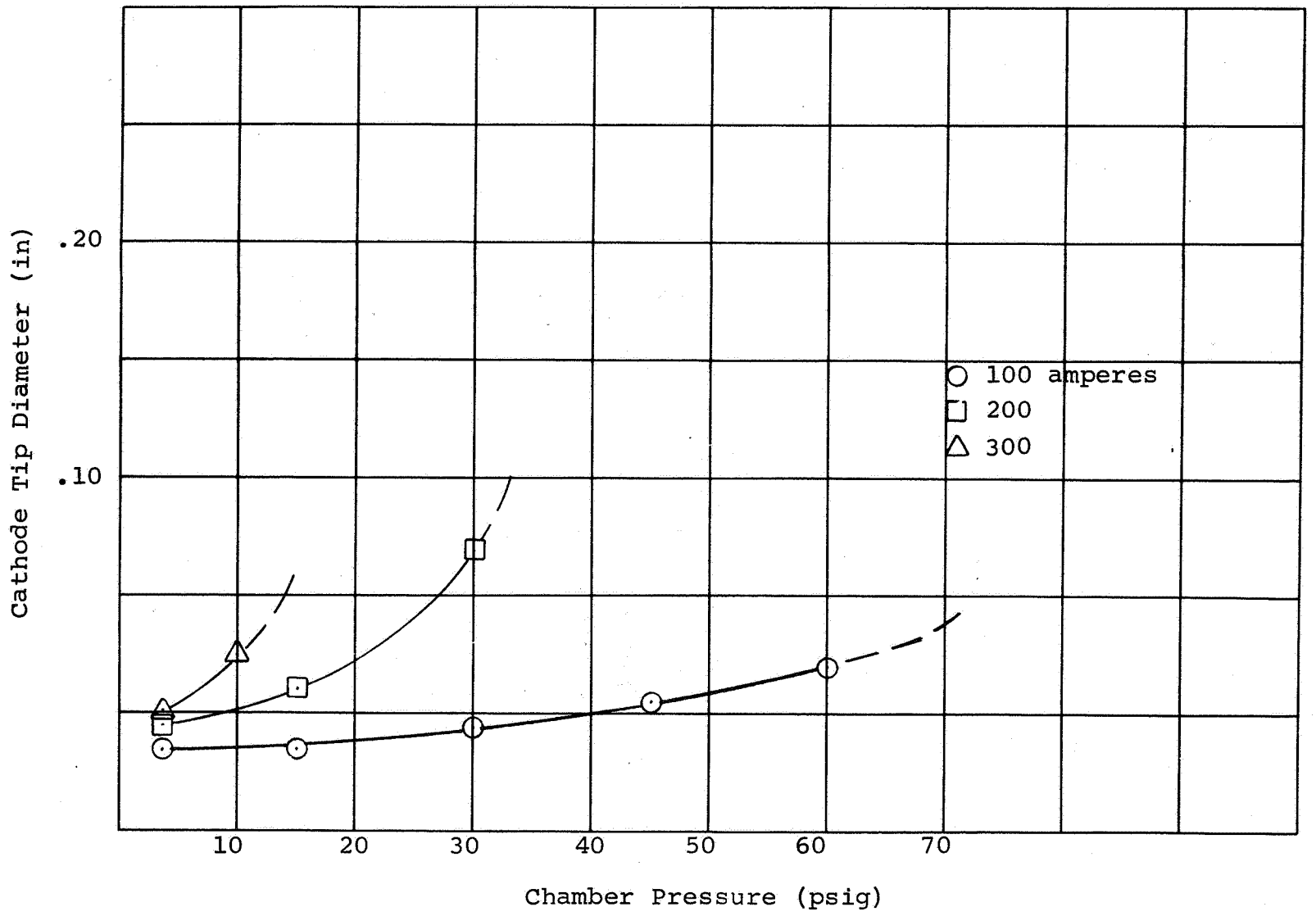

Figure 29: Cathode Diameter versus Chamber Pressure, 1/2-inch Thoriated Cathode

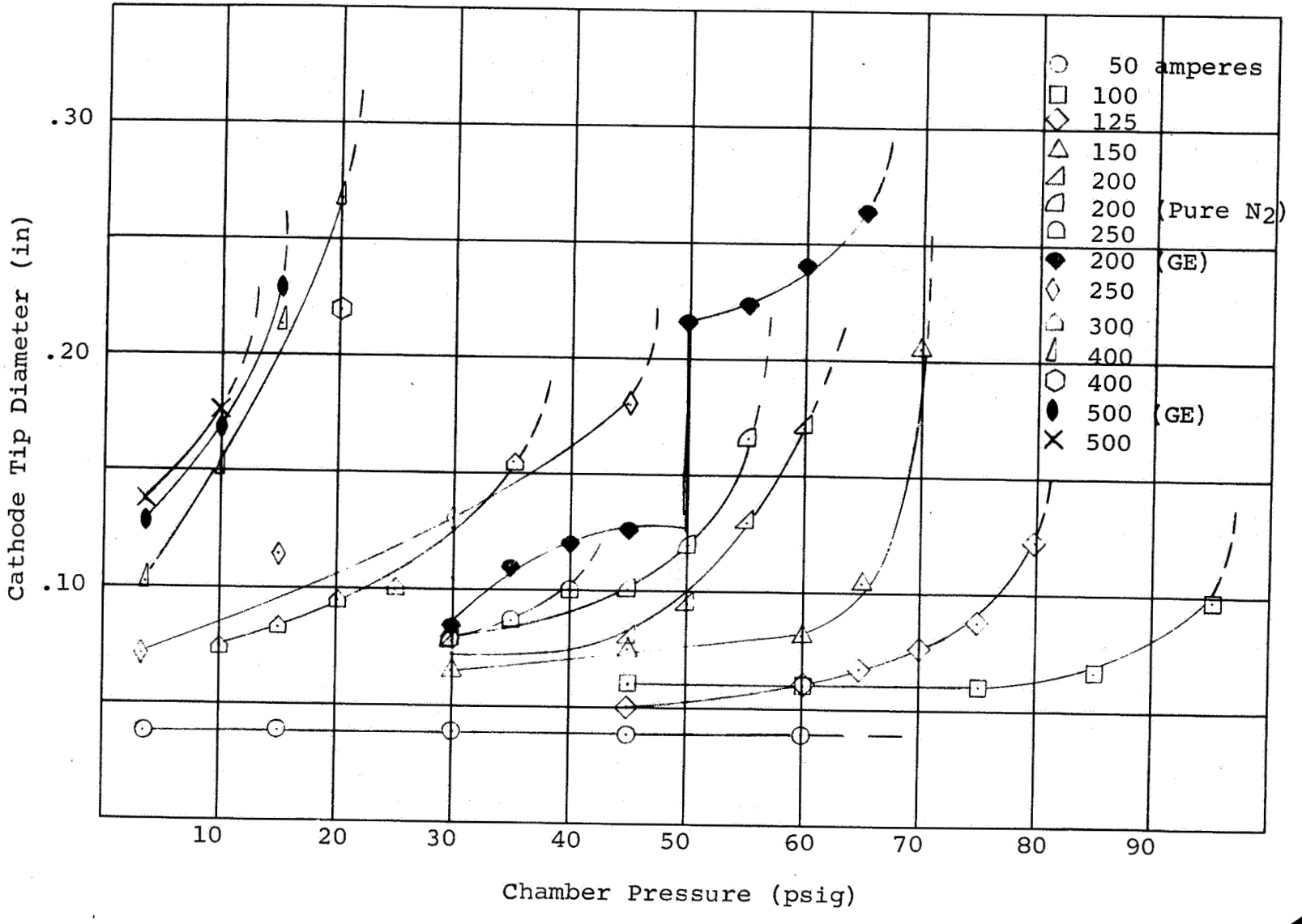

Figure 30: Cathode Diameter versus Chamber Pressure, 1-inch Thoriated-Cathode

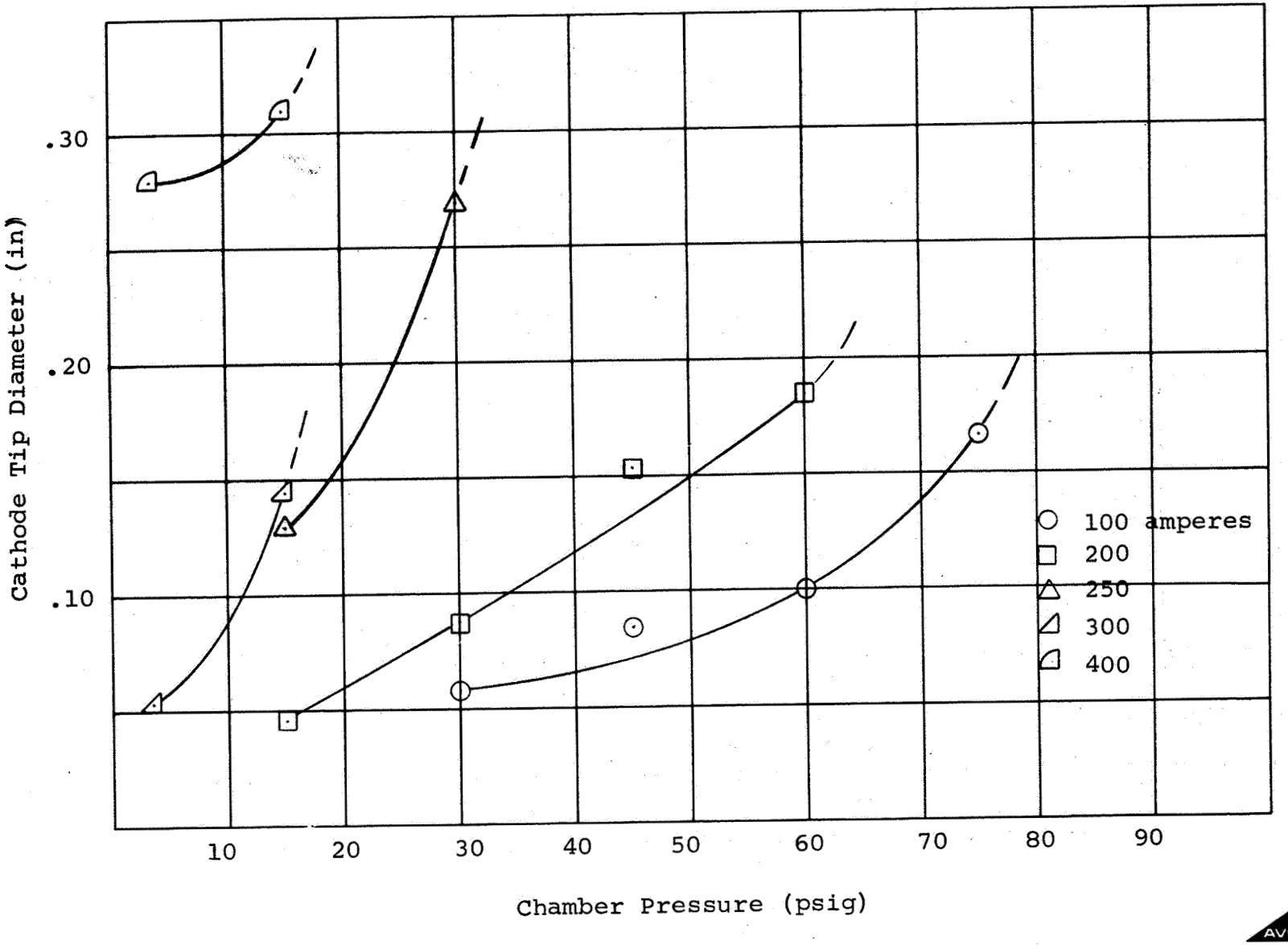

Figure 31: Maximum Pressure versus Cathode Diameter, Thoriated-Cathodes

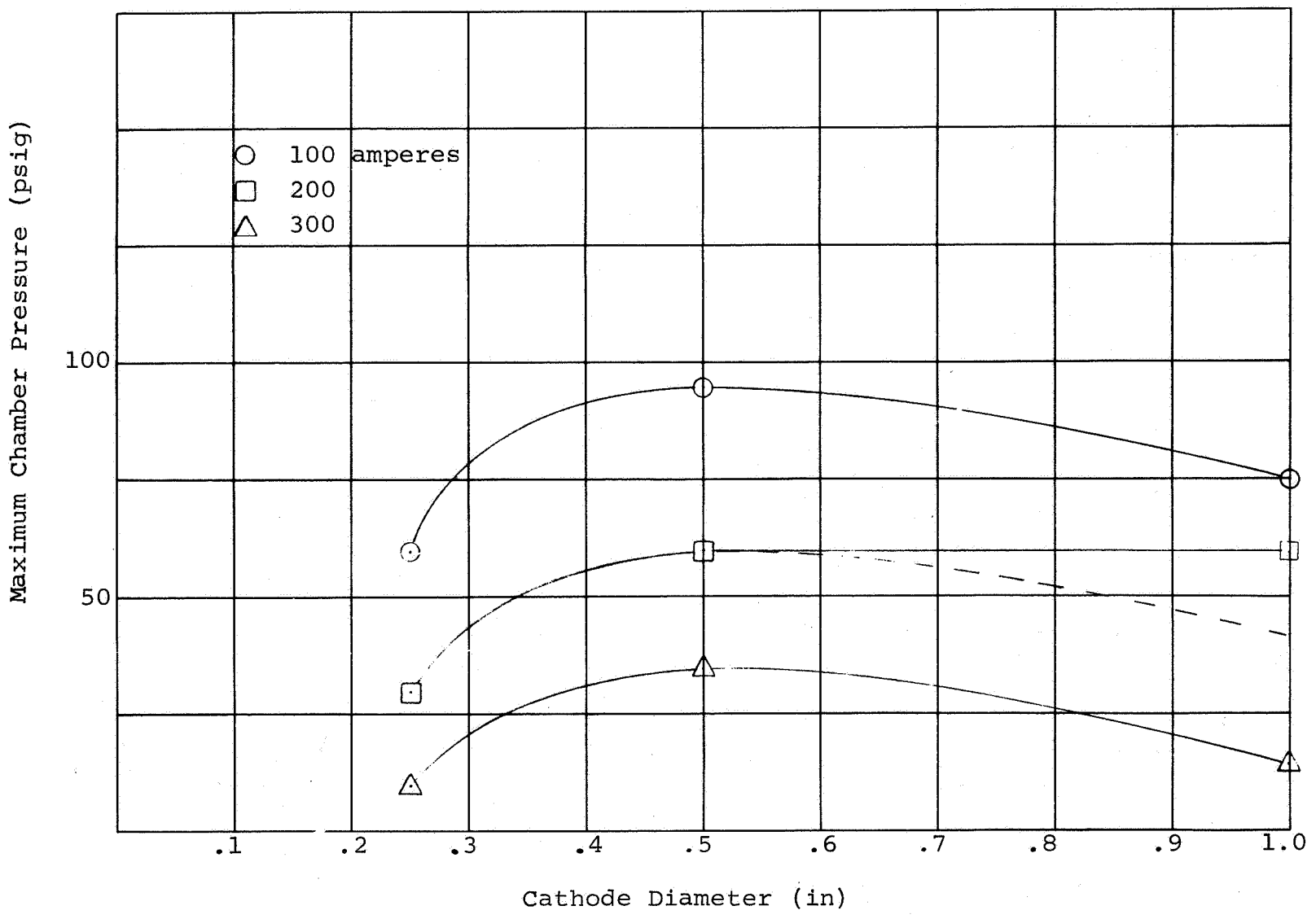

for each of the three arc currents. The improved performance evidenced in the increase from a 1/4-inch to a 1/2-inch diameter is anticipated on the basis of simple cross-section arguments. The increased cross-sectional area available for current flow and heat flow from the cathode tip to the cooled back surface of the cathode would suggest a lower tip temperature and less erosion at any given operating condition. The same argument would suggest that increased diameters above some value should have little or no beneficial effect upon performance, since cooling of the tip below melting temperature is all that would be desirable. The increase from ½-inch to 1-inch diameter could, by this argument, tend to over-cool the tip and prevent efficient thermionic emission.

This oversimplification is not proposed as an explanation for the observed phenomenon because there are, clearly other mechanisms operating as well. Because of the fixed geometry used for the tests, the increased cross-sectional area is accompanied by both an increased tip to cooled base length, as well as an increased surface area exposed to arc radiation. Each of these effects would act to oppose the effects of the increased cross-sectional area. A much more detailed discussion of these effects may be found, for example, in reference 7.

3. Effect of Cathode Shape

In this portion of the program, attempts were made to operate cathodes of geometrical configurations other than the cone-cylinder configurations discussed above. Two other configurations were examined. The first of these--a so-called "hollow" cathode configuration--is shown schematically in figure 32. Figures 33, 34 and 35 show photographs of three

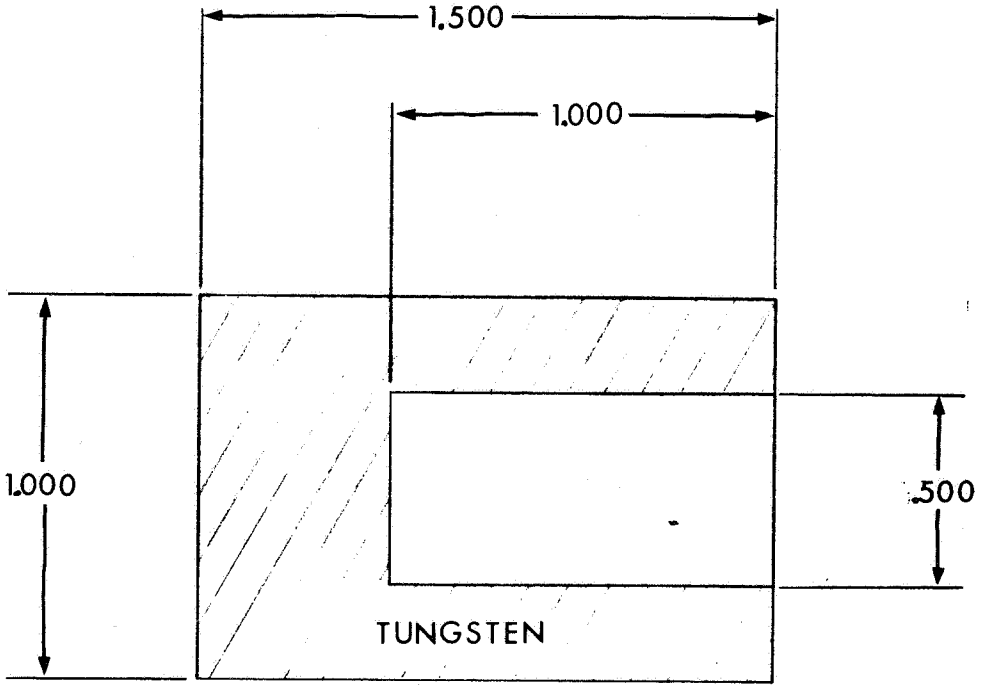


Figure 32: HOLLOW CATHODE

Figure 33: Photograph of Hollow Cathode After Testing, 500 A, 3.5 psig

Figure 34: Photograph of Hollow Cathode After Testing, 500A, 15 psig

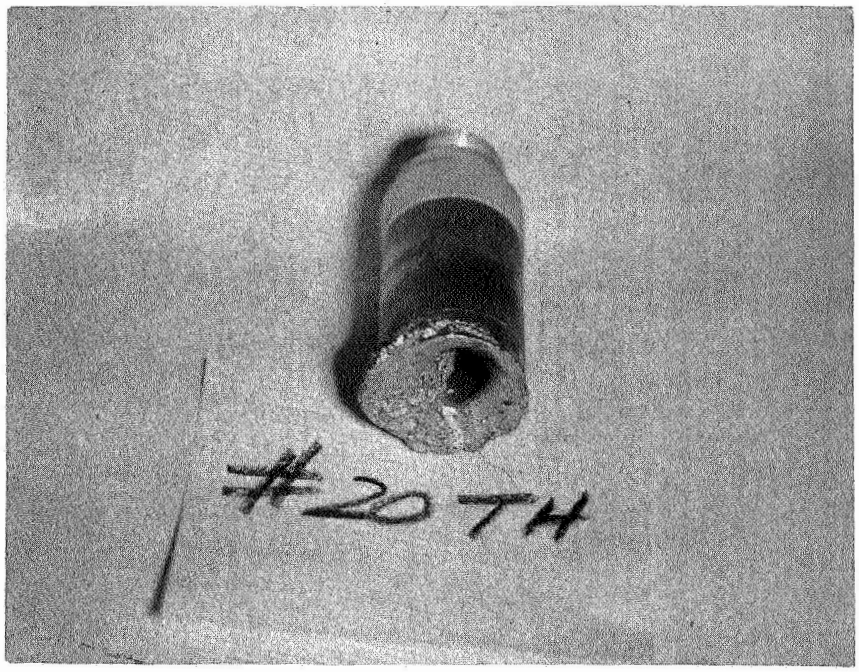


Figure 35: Photograph of Hollow Cathode After Testing, 500A, 30psig

such cathodes after 30 minutes of operation at a current level of 500 amperes and at pressures of 3.5, 15 and 30 psig, respectively. No equilibrium situation existed at the end of any of the 30 minutes tests of "hollow" cathodes.

Figure 36 shows a schematic of a "button" cathode, and figure 37 is a photograph of such a cathode prior to testing. All attempts to operate such cathodes were unsuccessful. There was evident a continuous erosion process throughout the test period, with the arc attachment wandering over the entire circumference of the tungsten to copper joint.

C. TEST RESULTS--FALL VOLTAGE

For each cathode material the heat power removed by the cathode cooling water has been measured. The ratio of this heat power to the arc current is a measure of the cathode fall voltage and depends upon the specific test gas used, the ambient gas pressure, and the cathode material, as well. The effective cathode fall voltage, defined as the removed heat power divided by the arc current, has been determined for each cathode test performed.

Figure 38 presents the effective cathode fall voltage as a function of chamber pressure for the ½-inch thoriated-tungsten cathodes operated in 100 to 500 ampere current range. The filled symbols on the figure represent the maximum pressure of cathode operation for each current level. Higher pressure level data points were obtained during catastrophic erosion operation and do not represent equilibrium conditions.

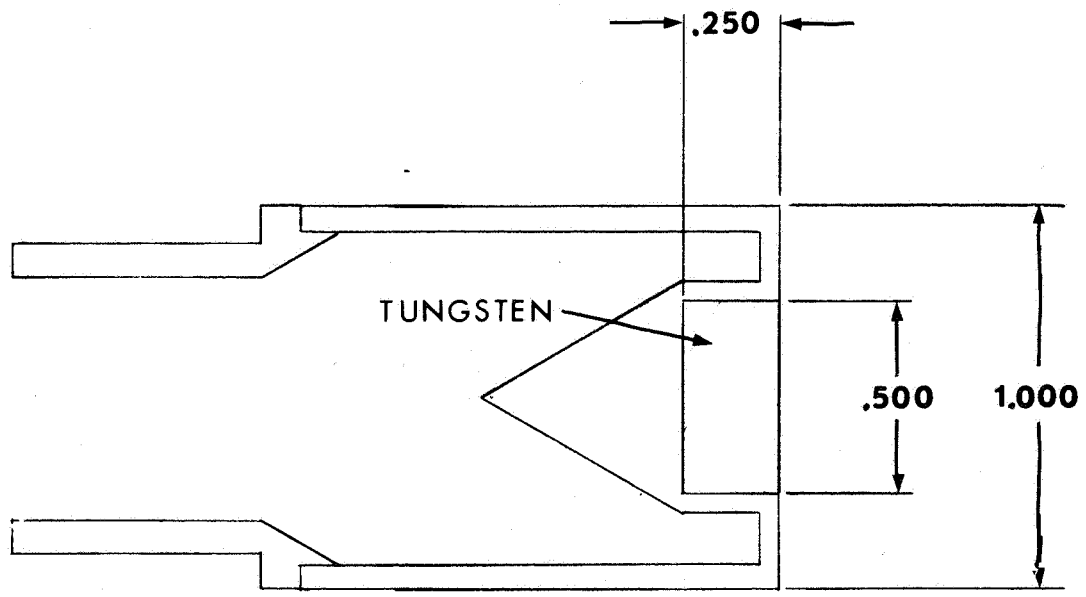


Figure 36: BUTTON CATHODE

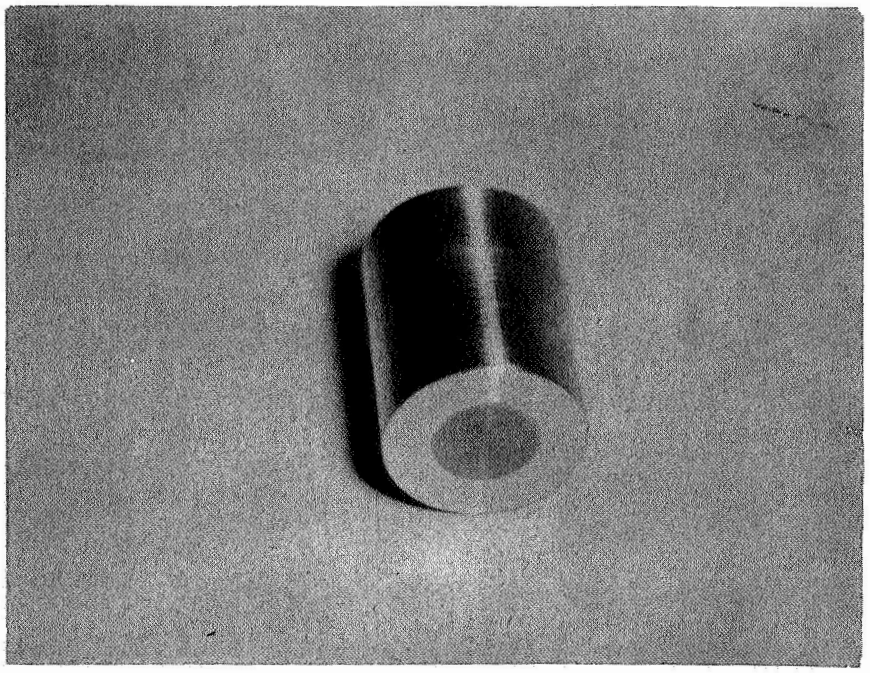

Figure 37: Photograph of Button Cathode Before Testing

Figure 38: Cathode Fall Voltage versus Chamber Pressure, Thoriated-Cathodes, ½-inch diameter

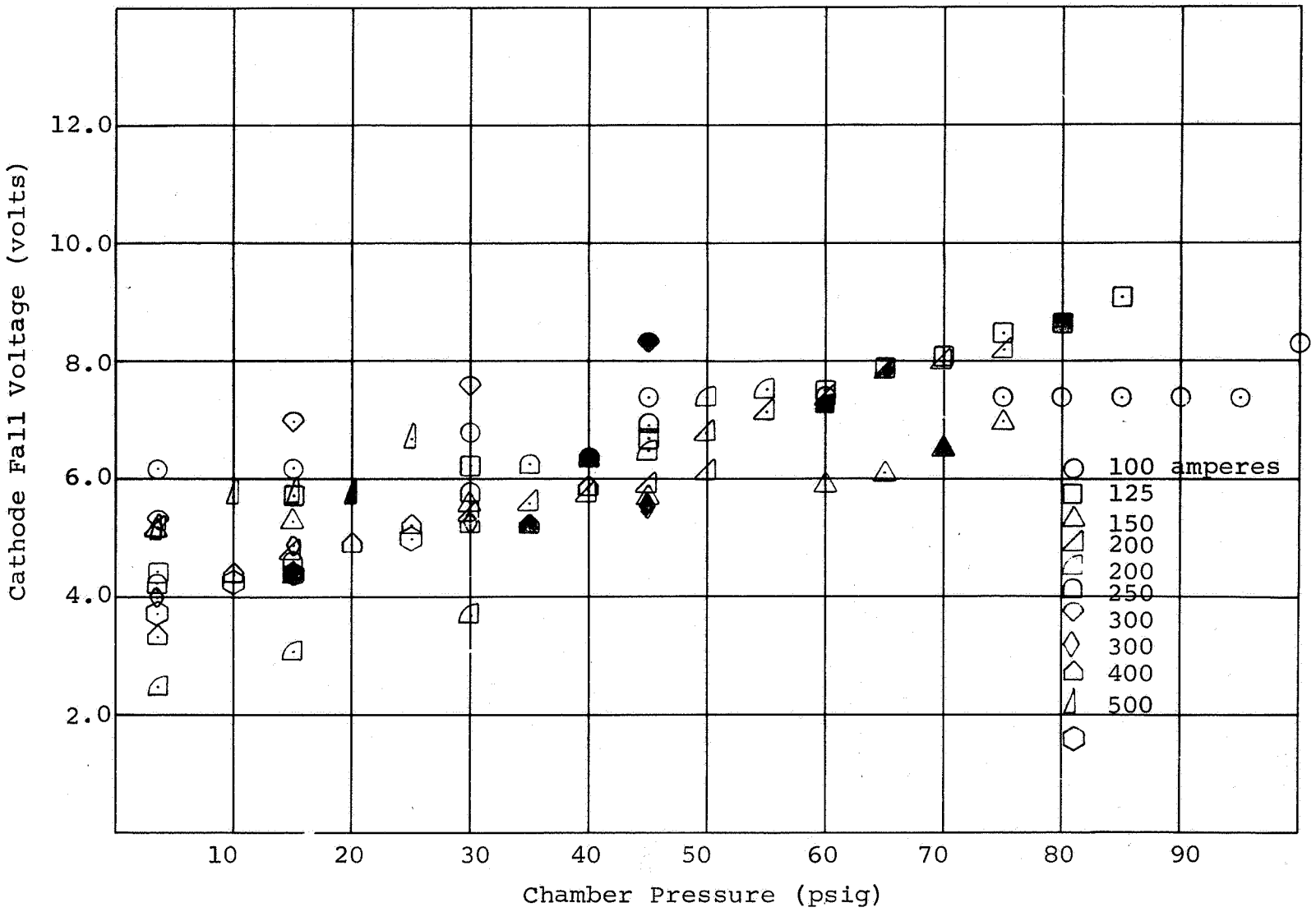

With the possible exceptions of one 250 ampere test and the 150 ampere test, all the data obtained may be fairly well represented by a single curve, with the effective fall voltage increasing in roughly linear fashion with increasing chamber pressure. For no test did the effective fall voltage rise much above 9 volts.

Figure 39 shows similar data accumulated with barium oxided-cathodes. For this material, also, the data points fall roughly upon a single curve with the same general behavior as the curve for the thoriated-cathodes. Figure 40 presents the data accumulated with barium calcium aluminated-cathodes. With the exception of the data for the 225 ampere test, the previous remarks are equally valid.

In order to compare the effective cathode fall voltages for the three materials with their performance characteristics, graphs of fall voltage versus chamber pressure have been plotted for several arc currents. Figures 41, 42, 43 and 44 show the effective fall voltages for the three materials at arc currents of 200, 250, 300 and 400 amperes, respectively. At 200 amperes arc current, both the barium oxided- and barium calcium aluminated-cathodes showd appreciably superior performance characteristics than the thoriated-cathodes (see figure 25). It is evident from figure 41 that for the same arc current, the cathode fall voltage was, at all pressures, higher for the thoriated-cathodes than for cathodes of the other two materials.

Figure 39: Cathode Fall Voltage versus Chamber Pressure, Barium Oxided Cathodes

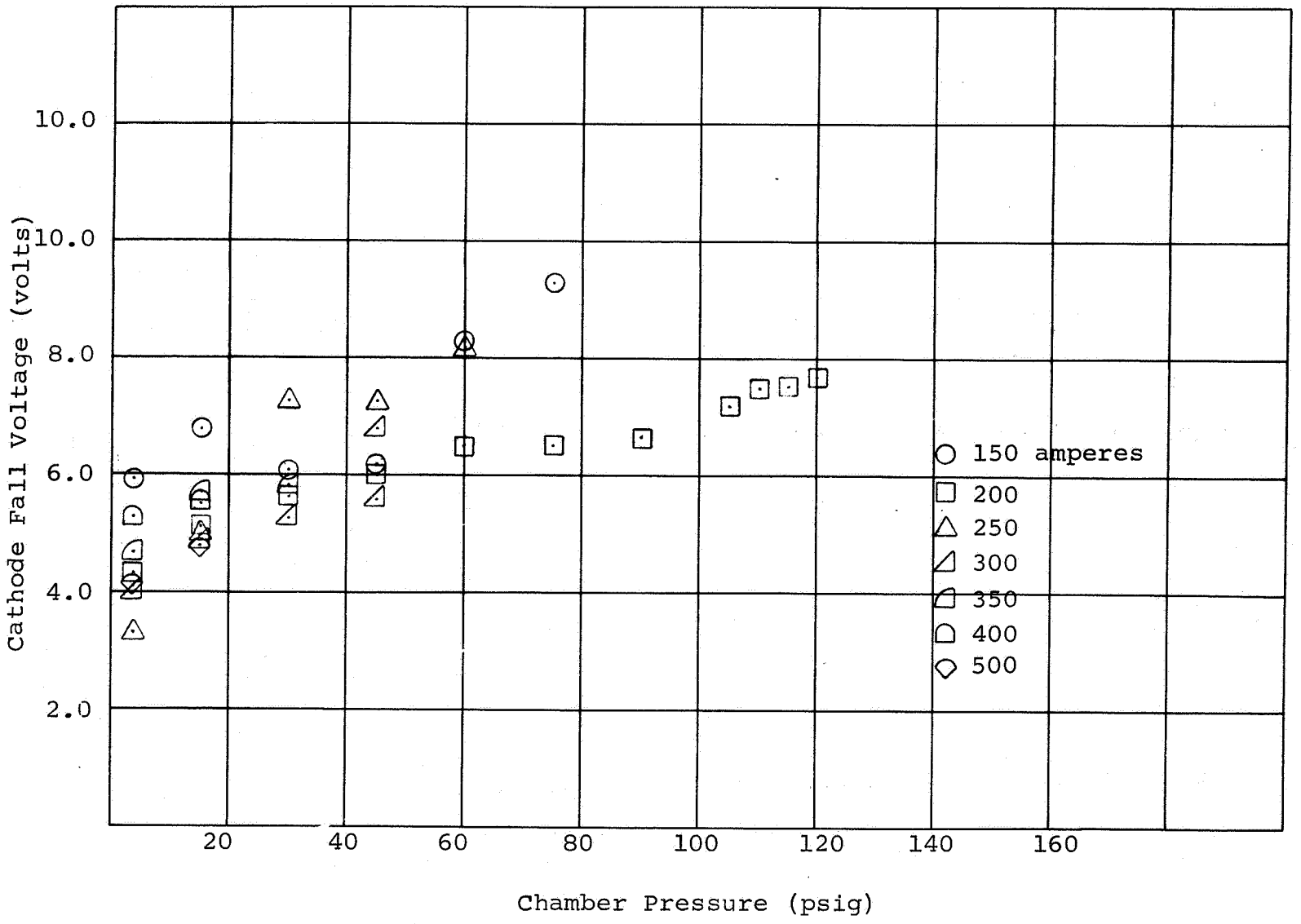

Figure 40: Cathode Fall Voltage versus Chamber Pressure, Barium Calcium Aluminated-Cathodes

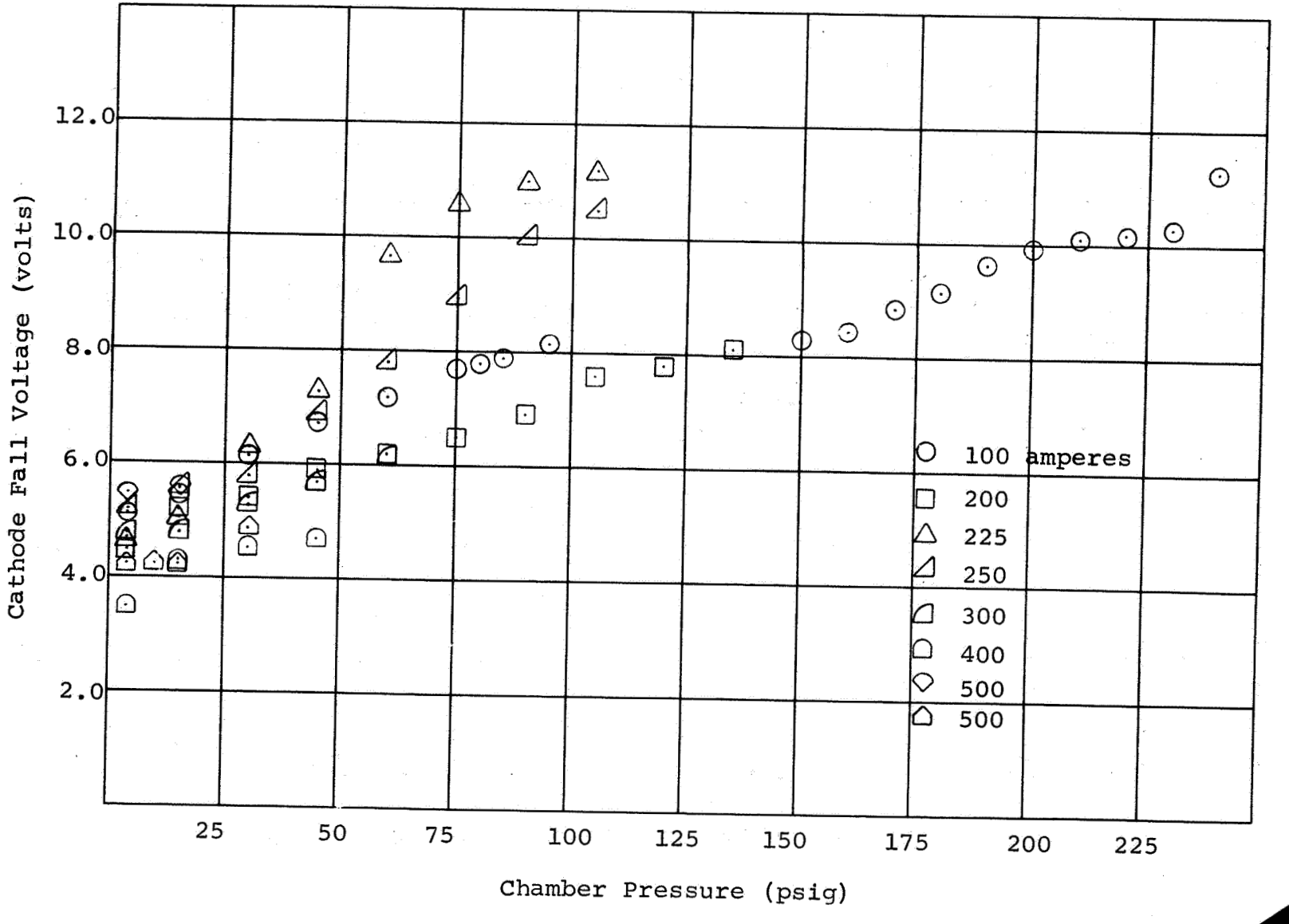

Figure 41: Cathode Fall Voltage versus Chamber Pressure, 200 amp.

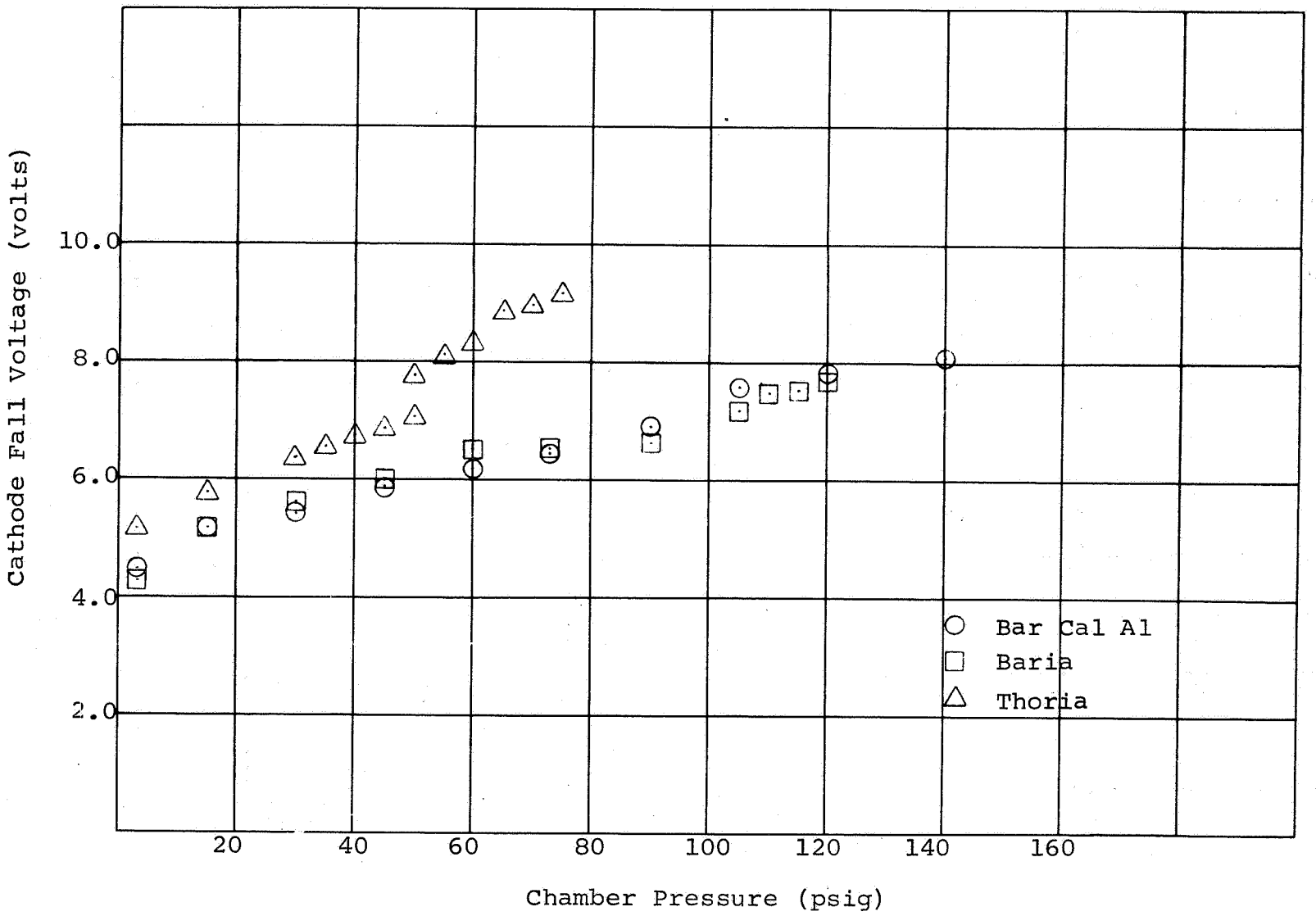

Figure 42: Cathode Fall Voltage versus Chamber Pressure, 250 amp.

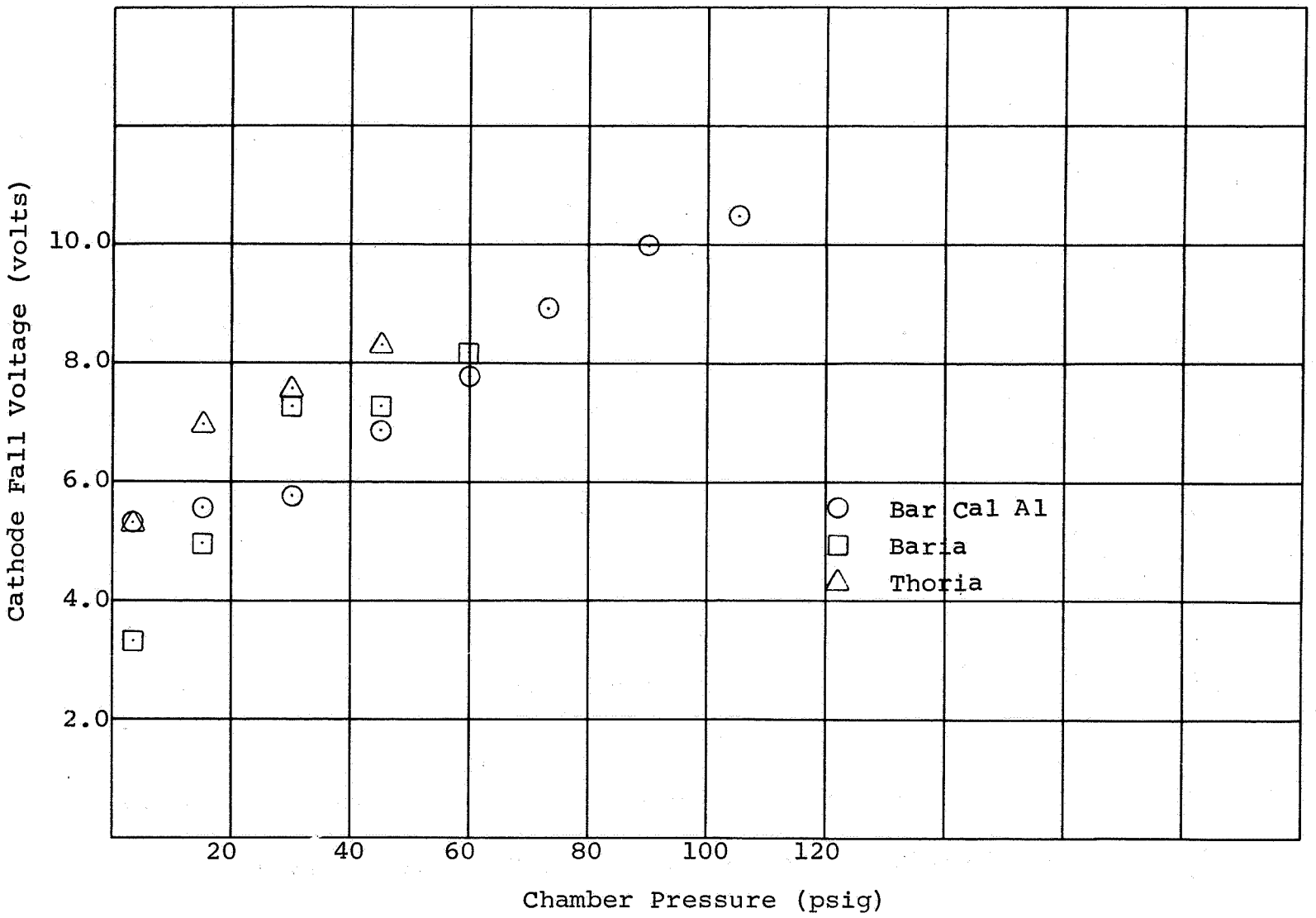

Figure 43: Cathode Fall Voltage versus Chamber Pressure, 300 amp.

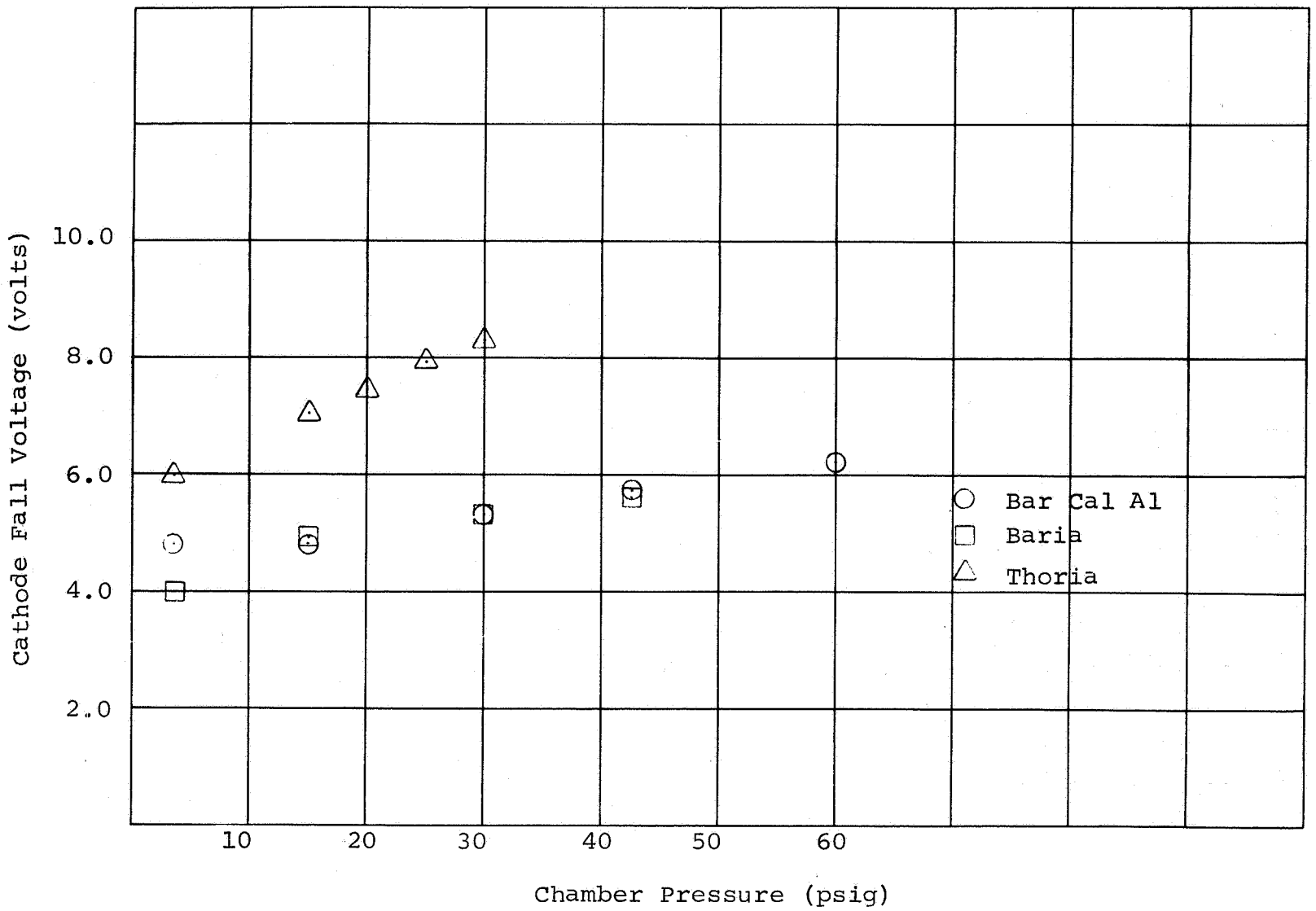

Figure 44: Cathode Fall Voltage versus Chamber Pressure, 400 amp.

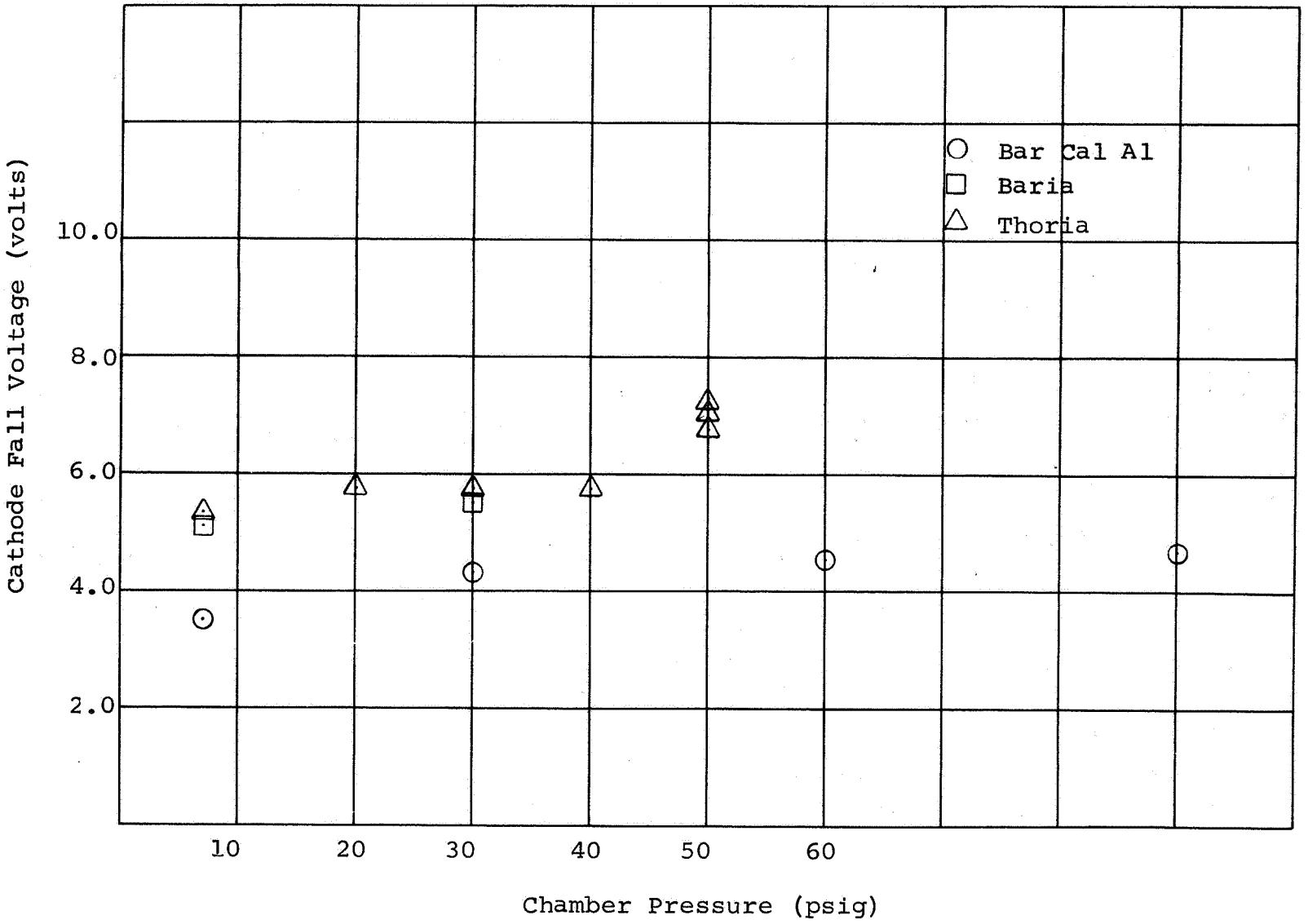

At the 400 ampere current level, the fall voltage for barium calcium aluminated-cathodes was considerably lower than for the other two materials (see figure 44). A comparison with figure 25 shows the relative performance at that current to be better, as well.

For each arc current, the barium calcium aluminated-tungsten cathodes operated at lower effective fall voltages, that is, less heat power had to be removed by the cooling water. No clearly discontinuous or sharp increases in effective fall voltages are apparent in the immediate vicinity of the critical pressure. There are also no specific fall voltage limits upon equilibrium cathode operation. In figure 38, for example, the spread in critical pressure fall voltages (filled symbols) may be seen to be as large as the range of operating values, themselves.

A comparison of the effective fall voltages for the different diameter thoriated-cathodes has been made, as well. Figures 45, 46 and 47 present plots of effective fall voltage as a function of chamber pressure for arc currents of 100, 200 and 300 amperes, respectively. At each arc current, the effective fall voltage rises slowly with pressure for each cathode diameter, but no outstanding dependence upon cathode diameter is observed.

## D. SUMMARY OF RESULTS

The most significant results obtained under the program are the following.

Figure 45: Cathode Fall Voltage versus Chamber Pressure
Thoriated-Cathodes, 100 ampere.

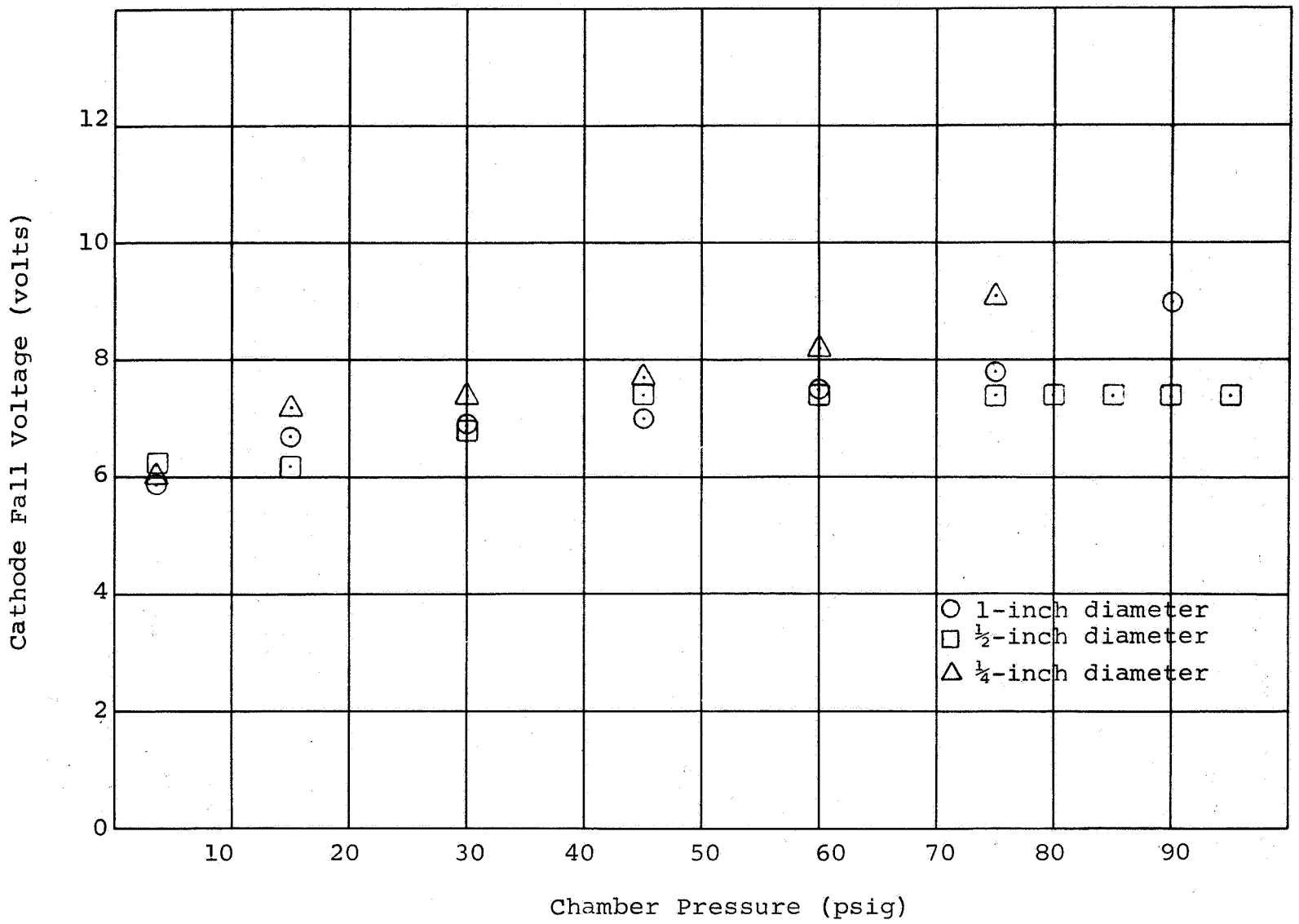

Figure 46: Cathode Fall Voltage versus Chamber Pressure, Thoriated-Cathodes, 200 ampere

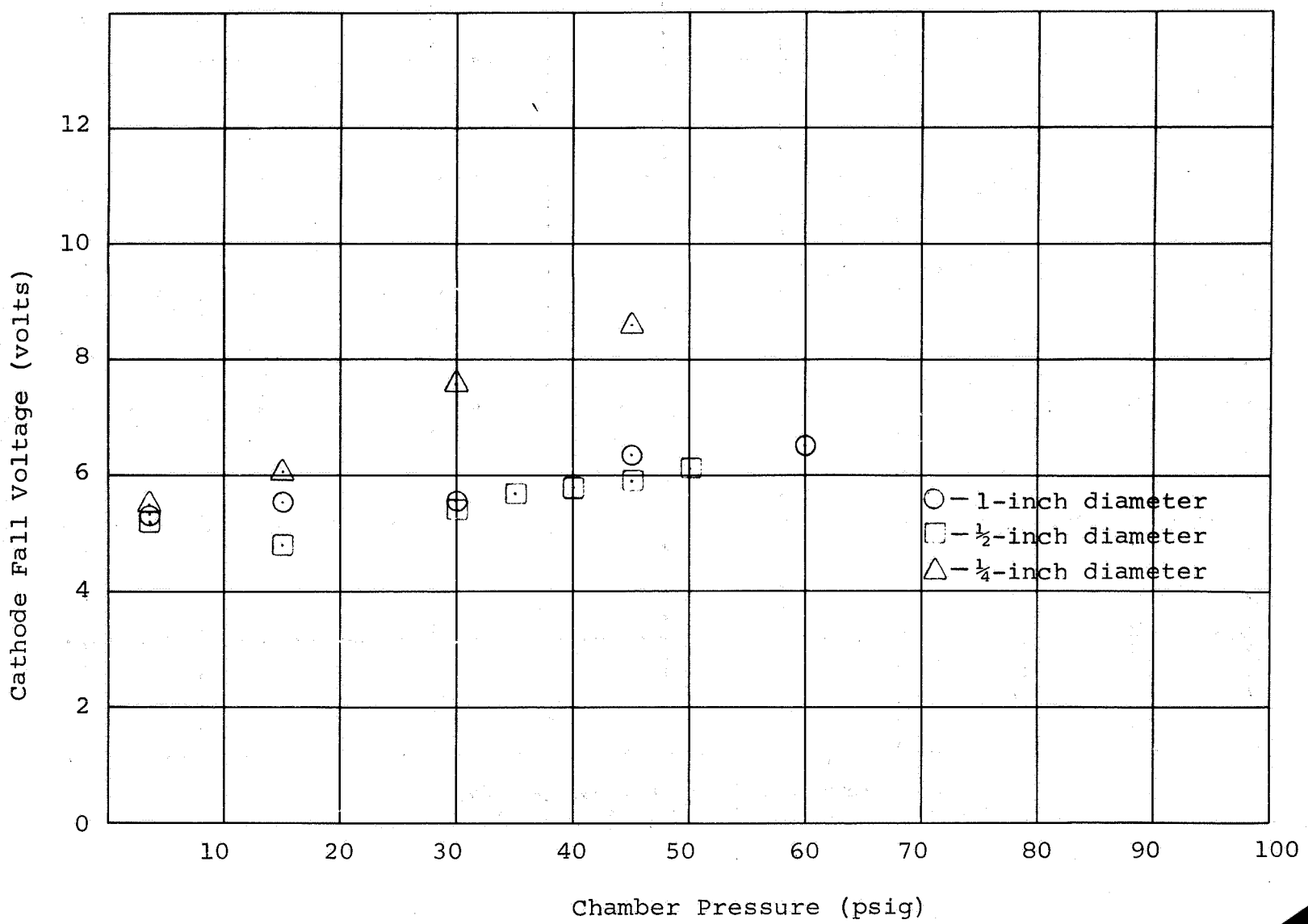

Figure 47: Cathode Fall Voltage versus Chamber Pressure
Thoriated-Cathodes, 300 ampere

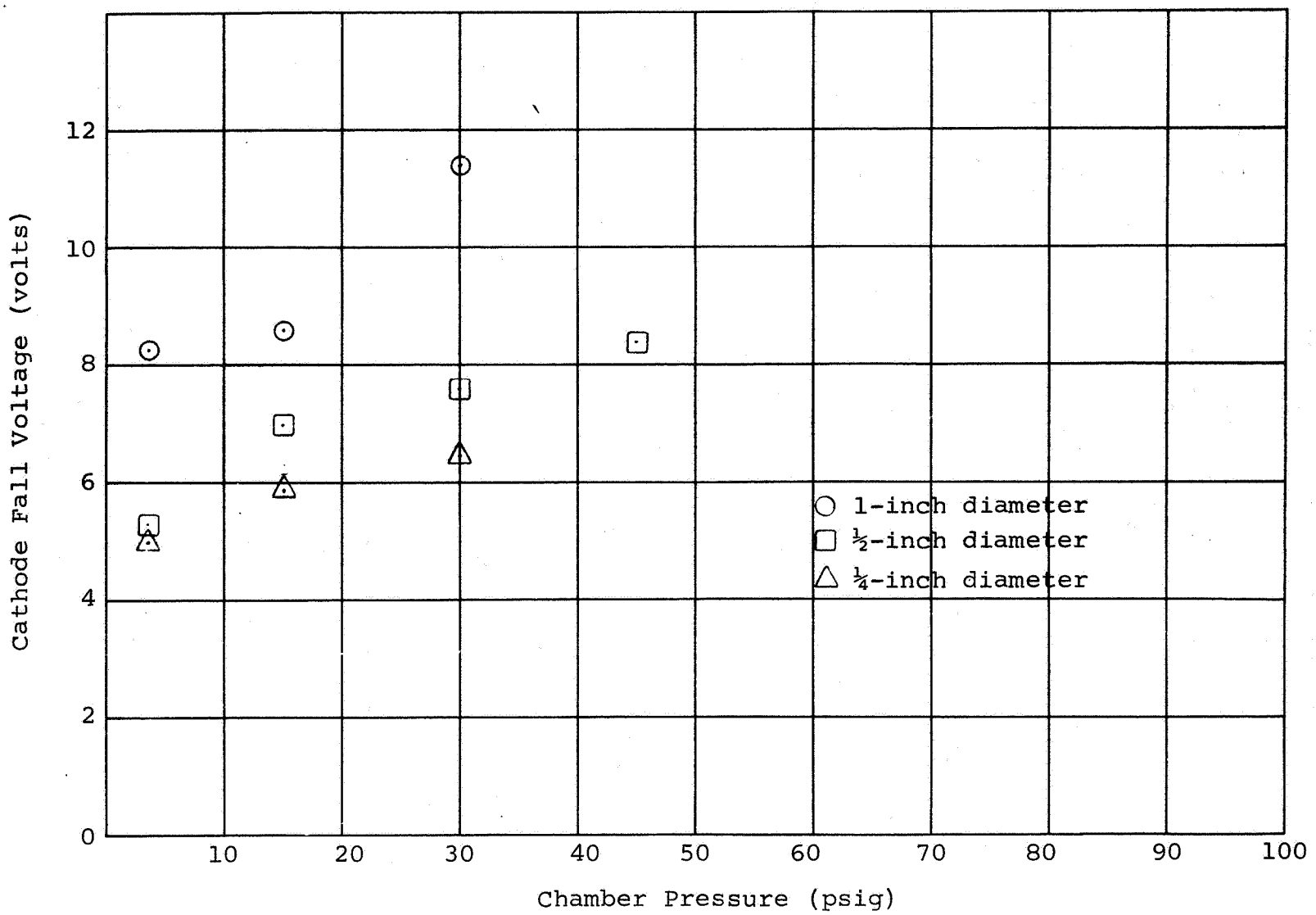

1. Barium Calcium Aluminate is an especially attractive additive to tungsten for use as a cathode material. Cathode performance is greatly enhanced at all current and pressure levels of arc operation utilized for this program. It is greatly superior in performance to either thorium oxide or barium oxide. The only disadvantage to its general use is the high cost required for the fabrication of the impregnated material. Its cost per cathode is of the order of 3 or 4 times the cost for thoriated-cathodes.

2. At current and pressure levels within the range of 100 to 500 amperes and 1 to 20 atmospheres of nitrogen, and for the fixed cone-cylinder geometry tested, the use of larger diameters does not always improve the performance characteristics of cathodes. The optimum performance characteristics were obtained for 1/2-inch diameter cathodes.

3. Several smaller diameter cathodes operated in parallel show a greater current-carrying capacity than a single cathode of the same cross-sectional area. For example, at a pressure level of 5 atmospheres, four 1/4-inch thoriated-cathodes can be operated, each carrying 100 amperes, for a total of 400 amperes. A single 1/2-inch thoriated cathode could carry only 200 amperes under the same conditions (see figure 25, for example). The cross-sectional cathode area for the two situations is the same.

## IV. CONCLUSIONS

Electrode phenomena in electric arcs have been studied experimentally and theoretically by a number of investigators. The literature on cathode fall voltages, current densities, and operating mechanisms is voluminous. Nevertheless, the design of cathodes has been carried out almost entirely on an empirical basis because no verified, quantitative theory capable of performance predictions of a cathode of given properties and geometry operating at a given current and pressure in a given gas has existed.

Several types of arc cathodes have been investigated experimentally. (See, for example, references 1-7). Much more work of a theoretical nature has been done, and a complete listing of the available literature would be an unrealistic project. However, references 7-29 may be used as a basic bibliography of the work done.

The present investigation has been almost entirely experimental in nature and has been directed towards providing a useful basis for rational design procedures for use at the higher currents and pressures encountered in high-energy wind tunnels for simulation of atmospheric reentry. The effort has been fruitful in providing information concerning the effects of different low work-function additives for cathodes. In particular, the use of barium calcium aluminate is highly recommended if cost is not a prohibitive factor in the material selection.

The results obtained have shown that, for a fixed geometrical configuration, there is apparently an optimum size cathode diameter for achieving good cathode performance characteristics. It is recommended that future experimental research areas should include the determination of the optimum cathode tip included angles and lengths for various cathode diameters. Such information would permit the design of high current and high pressure cathodes to proceed in a more rational fashion than the present empirical method allows.

## V. REFERENCES


1. Somerville, J. M., The Electric Arc, Methuen, London (1959).
2. Weinstein, R. H. and R. V. Hess, New Experiments with Hollow Cathode Discharges (for Application to Plasma Accelerators), Third Symposium on Engineering Aspects of Magnetohydrodynamics, Rochester, N. Y. (March 1962).
3. Zizka, E., Formation of Cathode Spots and Current Density Distribution, Air Force Systems Command report no. FTD-TT-63-1071 (1963).
4. Stebbins, R. A., An Experimental Study of a Hollow Cathode for Arc Devices, Master's thesis, School of Engineering, Air Force Institute of Technology, August 1964.
5. Grakov, V. and V. Hermoch, Behavior of Cathode Spots in a High Current Electric Discharge, Air Force Systems Command report no. FTD-TT-64-152 (1964).
6. Pfender, E., D. Y. Cheng and J. Doyle, Augmentation of the Total Current by Means of a Hollow Cathode, presented at AIAA Plasmadynamic Conference, Monterey, California, Paper no. 66-191 (1966).
7. Bade, W. and J. Yos, Theoretical and Experimental Investigation of Arc Plasma Generation Technology, Part II, Vol. I, Avco report no. RAD-TR-63-11 (1964).
8. Weizel, W. and W. Thouret, Lichtbögen mit und ohne Brennfleck, Z. Physik 131, 170-184 (1952).

9. Ecker, G., Die Erscheinung des Beweglichen Einfach und Mehrfachbrennflecks an der Kathode des Elektrischen Lichtbögens, Z. Physik 136, 556-572 (1954).

10. Ecker, G., Electrode components of the arc discharge, Ergeb. exakt. Naturwiss. 33, 1-104 (1961).

11. Mackeown, S. S., (The) Cathode drop in an electric Arc, Phys. Rev. 34, 611-614 (1929).

12. von Engel, A. and A. E. Robson, (The) Excitation theory of arcs with evaporating cathodes, Proc. Roy. Soc. (London) A242, 217-236 (1957).

13. Hernqvist, K. G., Emission mechanism of cold-cathode arcs, Phys. Rev. 109, 636-646 (1958).

14. Dolan, W. W. and W. P. Dyke, Temperature-and-field emission of electrons from metals, Phys. Rev. 95, 327-332 (1954).

15. Murphy, E. L. and R. H. Good, Jr., Thermionic emission, field emission and the transition region, Phys. Rev. 102, 1464-1473 (1956).

16. Nottingham, W. B., Thermionic Emission, In: Handbuch der Physik, vol. 21, Springer - Verlag, Berlin (1956), p. 6-7, 32.

17. Hagstrum, H. D., Auger ejection of electrons from tungsten by noble gas ions, Phys. Rev. 104, 317-318 (1956).

18. Holm, R., (The) Vaporization of the cathode in the electric arc, J. Appl. Phys. 20, 715-716 (1949).

19. Müller, G. and W. Finkelnburg, Über den Kathoden-und Anodenfall eines Kohlelichtbogens hoher Stromstärke, Naturwissenschaften 42, 294 (1955).

20. Rich, J. A. Resistance heating in the arc cathode spot zone, J. Appl. Phys. 32, 1023-1031 (1961).

21. Bauer, A., Untersuchungen uber den Kathodenfall in den Übergangsbereichen vom Thermobogen zum Feldbogen und vom Bogen zur Glimmentladung, Ann. Physik 18, 387-400 (1956).

22. Lee, T. H., T-F theory of electron emission in high-current arcs, J. Appl. Phys. 30, 166-171 (1959).

23. Lee, T. H., Energy distribution and cooling effect of electrons emitted from an arc cathode, J. Appl. Phys. 31, 924-927 (1960).

24. Lee, T. H. and A. Greenwood, Theory for the cathode mechanism in metal vapor arcs, J. Appl. Phys. 32, 916-923 (1961).

25. Lee, T. H. and A. Greenwood, Space Charge and Ionization Regions Near the Arc Cathode, Aerospace Research Laboratories report no. ARL-163 (1963).

26. Lee, T. H., A. Greenwood, W. D. Breingan and H. P. Fullerton, Voltage Distribution, Ionization, and Energy Balance in the Cathode Region of an Arc, Aerospace Research Laboratory report no. ARL64-152 (1964).

27. Lee, T. H., A. Greenwood, W. D. Breingan and H. P. Fullerton, Analytical Study of the Physical Processes in the Cathode Region of an Arc, Aerospace Research Laboratory report no. ARL66-0065 (1966).

28. Briggs, D. C., Transient Temperature Distribution in Electrodes with Moving Arcs, Aerospace Research Laboratories report no. ARL64-32 (1964).

29. Soehngen, E. E., Energy Exchange Phenomena in Electric Arcs, presented at National Congress of the ASME, October 1962.

DISTRIBUTION

External

| Addressee | Number of Copies |
| --- | --- |
| NASA/Ames Research Center<br>Moffett Field, California 94035<br>Attention: Patent Counsel | 2 |
| NASA/Ames Research Center<br>Moffett Field, California 94035<br>Attention: Technical Information Division | 33 |

DISTRIBUTION

Internal

W. Bade
S. Bennett (5)
L. Cass
G. Enos (3)
M. Goriansky
R. John
R. Krauss
A. Malliaris
M. Malin
W. Powers
C. Simard
A. Tuchman (20)
J. Yos
Central Files